Tampereen yliopisto

Lotta Kääriäinen

OPTIMIZATION OF THIN FILMS PREPARATION FOR THE LIGHT-RESPONSIVE CELL CULTURE PLATFORM

TIIVISTELMÄ

Kudokset ovat jatkuvasti muuttuvia biologisia mikroympäristöjä, jotka muodostuvat soluista ja niitä ympäröivästä soluväliaineesta. Tällainen dynaaminen ympäristö vaikuttavaa voimakkaasti solujen toimintaan, esimerkiksi solujen erilaistumiseen ja migraatioon. Perinteiset, kaksiulotteiset soluviljelyalustat eivät pysty jäljittelemään solujen luonnollista, dynaamista ympäristöä. Tämä muuttaa viljeltyjen solujen toimintaa verrattuna luonnollisessa mikroympäristössään elävien solujen toimintaan. Näin ollen ärsykkeisiin reagoivia, dynaamisia soluviljelyalustoja tarvitaan kudosten luontaisten ominaisuuksien jäljittelemiseen *in vitro* -olosuhteissa.

Isomäki *et al.* ovat luoneet valo-ohjattavan soluviljelyalustan, jolla voidaan reversiibelisti ohjata epiteelisolujen orientoitumista alustan pintatopografian avulla. Alusta koostuu ohuesta atsobentseenijohdannaisesta Disperse Red 1 -lasista (DR1-lasista) sekä ohuesta polydimetyylisiloksaanikerroksesta (PDMS-kerroksesta). Alusta vaatii kuitenkin optimointia, sillä DR1-lasikalvot ovat epätasaisia, ja kalvojen paksuus vaihtelee sekä saman kalvon sisällä että eri kalvojen välillä. Nämä erot vaikuttavat kalvojen optisiin ominaisuuksiin, mikä vaikeuttaa alustasta kerättävän tutkimusdatan tulkintaa ja vertailua biologisissa sovelluksissa. Lisäksi alustan optimoiminen on välttämätöntä alustan kaupallistamiseksi tulevaisuudessa.

Tutkimuksen tavoitteena oli optimoida Isomäen *et al.* luoman valo-ohjattavan soluviljelyalustan DR1-lasien valmistusprotokolla, jotta lasikalvot olisivat tasalaatuisia ja protokolla toistettavissa. Kalvoissa käytettävä liuotin, DR1-lasiliuoksen valmistus sekä varsinainen kalvojen valmistaminen spin coating -tekniikalla optimoitiin korkealaatuisten kalvojen valmistamiseksi.

Optimoinnin seurauksena kalvoista saatiin tasalaatuisia ja valmistusprotokollasta toistettava. Kalvojen ulkoasu parani merkittävästi, ja niissä esiintyvät materiaalikeräntymät- sekä epätasaisuudet saatiin eliminoitua. Lisäksi kalvojen absorptiospektrien välinen maksimivirhe pieneni yli 90 %. Tulosten mukaisesti optimoitujen DR1-lasikalvojen laatu on riittävän hyvä, jotta niitä voidaan tulevaisuudessa käyttää solujen ja materiaalin välisten vuorovaikutusten, sekä solujen käyttäytymisen tutkimiseen dynaamisessa ympäristössä.

Avainsanat: Atsobentseeni, valo-ohjattava, soluviljely, biomateriaali, spin coating -tekniikka

Tämän julkaisun alkuperäisyys on tarkastettu Turnitin OriginalityCheck –ohjelmalla.

ABSTRACT

Tissues are constantly changing microenvironments composed of cells and the extra-cellular matrix (ECM). This dynamic environment regulates the cell functions, such as differentiation and migration. Traditional 2D cell culture platforms lack the natural, dynamic characteristics of tissue, which alters the behaviour of cultured cells compared to the behaviour of cells living in their natural microenvironment. Thus, stimuli-responsive, dynamic cell culture platforms are needed for better mimicry of natural tissues *in vitro*.

Isomäki *et al*. have presented a light-responsive cell culture platform for reversible cell guidance. The platform consists of a thin spin coated film of azobenzene-based Disperse Red 1 - glass (DR1-glass) covered with a thin polydimethylsiloxane (PDMS) coating. This bilayer structure can be reversibly photopatterned, and the surface topography of the material is used for guiding focal adhesion alignment and orientation of epithelial cells cultured on top of the platform. However, the thin DR1-glass films are inhomogeneous, and the film thickness varies between separate films and at different spatial locations inside a single film. Such differences affect the optical properties of the material. Hence, the DR1-glass film preparation protocol needs to be optimized for reliable comparison and interpretation of the data collected from the platform. Additionally, the optimization is inevitable for prospective commercialization of the platform.

The aim of this research was to optimize the DR1-glass thin films preparation protocol to produce high-quality and reproducible films for light-responsive cell culturing. The optimization included the solvent used for DR1-glass films, preparation of the spin coating solution and the actual sample preparation by spin coating.

As a result of the optimization, the appearance of the films was massively improved, and the material aggregates and swirls on the films were eliminated. The maximum standard error of the absorption spectra of the films decreased by over 90 %. The optimized DR1-glass films are now uniform and the sample preparation protocol reproducible. Accordingly, these high-quality films can be used in research of cell-material interactions and cell behaviour in dynamic environments.

Keywords: Azobenzene, light-responsive, cell culture, biomaterial, spin coating

CONTENTS

ABBREVIATIONS AND SYMBOLS

AFM	atomic force microscopy
A	absorbance
BSA	bovine serum albumin
d	diameter
DAPI	4',6'diamidino-2-phenylindole
DCM	dichloromethane
DE	diffraction efficiency
DHM	digital holographic microscopy
DMF	dimethylformamide
DR1	Disperse Red 1 azo die
DR1-glass	Disperse Red 1 -molecular glass
EBL	electron beam lithography
ECM	extra-cellular matrix
FAK	focal adhesion kinase
FIB	focused ion beam
He-Ne laser	helium-neon laser
MDCK II	Madin-Darby canine kidney type II cells
MilliQ	highly pure, deionized water
PBS	phosphate-buffered saline
PDMS	polydimethylsiloxane
PFA	paraformaldehyde
pFAK	phosphorylated focal adhesion kinase
Pol	polarization
PP	polypropylene
P_0	output power of a probe beam
P_1	power of the 1st-order beam
rpm	rounds per minute
SRG(s)	surface-relief grating(s)
t	thickness
THF	tetrahydrofuran
UV	ultraviolet, a form of electromagnetic radiation with a wavelength of 10-400 nm
Vis	visible light, a form of electromagnetic radiation with a wavelength of 400-700 nm
wt-%	weight percent
θ	angle in which the writing beam hits a mirror in Lloyd's mirror setup
α	attenuation factor between absorbance and thickness of the spin coated film
ω	rotational speed
Λ	lateral period for SRGs
λ	wavelength
% v/v	volume percentage
2D	2-dimensional
3D	3-dimensional

1. INTRODUCTION

Tissues are dynamic and very complex microenvironments composed of cells with their internal cytoskeletal filament structures, along with the extracellular matrix (ECM). The ECM is a network consisting of macromolecules, such as collagen and elastin, and other compounds secreted by the cells. The ECM provides support and strength to tissues and works as a connection between cells. [1] Cells are constantly interacting with surrounding cells as well as the ECM and signaling with one another. These interactions are playing a major role in several cell functions, including migration, adhesion, differentiation and even apoptosis [2]. The previously mentioned functions also take part in complicated physiological processes, for instance tissue repair [3].

Cell culture refers to a process of growing cells under controllable *in vitro* conditions. It is one of the key tools used in cellular and molecular biology, and used in wide range of applications, such as studying physiology and modelling numerous diseases. So far, cell culture experiments have been primarily executed on two-dimensional (2D) platforms, such as commercially available Petri dishes. These platforms are easy to use, and they promote high cell viability. [4] However, traditional cell cultures have limited applicability for understanding and controlling cell behavior, since they often lack the dynamic and complex characteristics of tissue. Unlike the ECM, these platforms do not interact with the cells growing on top, and the loss of the environmental cues and the cell-ECM inter-actions often lead to alterations in cell behavior [4]. Consequently, new stimuli-respon-sive materials and dynamic substrates and matrices are being studied and developed for better mimicry of the body and its functions. A variety of stimuli, such as temperature, light, pH and magnetic fields, are being investigated for their potential to modify the prop-erties, structures and interactions of a material [5].

Light-responsive materials are promising alternatives for cell culture use for multiple rea-sons [6]. The properties of light, such as wavelength, polarization, and intensity, can be easily and precisely controlled [3]. Light can be introduced to the targets at singe-cell level with relatively low impact on cell behavior [7]. Moreover, light-responsive com-pounds, such as azobenzenes, have been widely studied and used in, e.g., photonic applications, such as microlens arrays or near-field sensing and imaging instruments [8].

In a recent publication, Isomäki *et al*. have presented a light-responsive cell culture platform for reversible cell guidance. The platform consists of a thin spin coated film of azobenzene-based Disperse Red 1 -glass (herein referred to as DR1-glass) covered with a thin polydimethylsiloxane (PDMS) coating. These films form a bilayer structure, which can be photopatterned and used for guiding focal adhesion alignment and orientation of epithelial cells cultured on top of the material. [3] This dynamically controlled photo-responsive cell culture platform is promising for further dynamic *in vitro* studies of cell interactions with the material and other cells. Still, there are a few challenges considering the platform that need to be solved for using it in biological applications.

One of the biggest challenges of the light-responsive cell culture platform presented by Isomäki *et al.*, is the inhomogeneity of the DR1-glass films. The film thickness varies between separate samples and at different spatial locations on a single sample substrate. Such inhomogeneities lead to differences in the optical properties of the samples. In other words, the samples are not uniform nor the sample preparation protocol reproducible enough for excluding sample dependences of cell behavior and detecting finer differences in cell-related parameters. Additionally, in light of prospective commercialization purposes of the platform, the sample preparation protocol needs to be reproducible and the samples uniform to ensure high quality of the product.

The aim of this thesis is to optimize the DR1-glass thin films preparation protocol to produce high-quality and reproducible samples for light-responsive cell culturing. Optimization is inevitable for reliable comparison and interpretation of the data collected from the platform.

The optimization includes the solvent used for DR1-glass samples, preparation of the spin coating solution along with the actual spin coating process. The spin coating process consists of dispensing the liquid material onto a substate, spinning the substrate on high speed and evaporation of the solvent [9]. Parameters considering these phases are examined individually to produce optimal film quality. The results of the optimization process are used for compiling the optimized manufacturing protocol for DR1-glass thin films. Furthermore, a tool for finding proper parameters for preparation of DR1-glass film with a certain thickness is presented. Finally, error sources in sample preparation as well as scaling up the preparation process are briefly discussed.

2. BACKGROUND

In this chapter, the background information relevant for understanding the research methodology and results, is presented. The chapter is divided into five separate sections: 2.1 Azobenzene compounds, 2.2 Spin coating, 2.3 Optical setup for the SRG inscription, 2.4 Cytocompatibility of a material and 2.5 Light-responsive cell culturing.

2.1 Azobenzene compounds

Azobenzene is an aromatic molecule consisting of two azo-linked phenyl rings. In the azo-linkage (-N=N-), two nitrogen atoms are connected by a covalent double bond. Due to this chemical structure and conversion of the -N=N- bond, azobenzene has two isomers – thermodynamically stable *trans* isomer and metastable *cis* isomer. The isomerization between these conformations can be reversibly induced by exposing the molecule to certain wavelengths of light. [10] In other words, azobenzene is a photoswitchable compound. For an unsubstituted azobenzene, the conversion from *trans* form to *cis* form can be induced using a UV-wavelength between 320 and 350 nm, whereas the molecule will convert back to *trans* form with a wavelength of 400 to 450 nm. Alternatively, the conversion back to *trans* form occurs thermally. [11] The structure and photoisomerization of azobenzene is shown in figure 1.
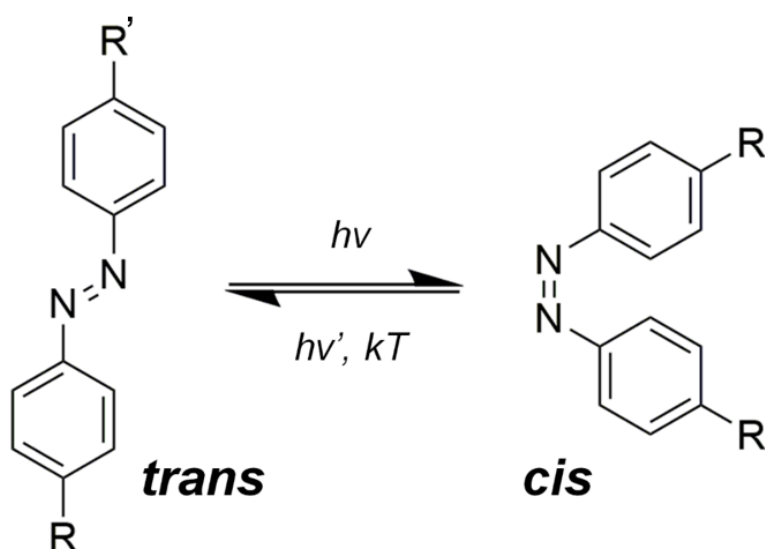

Figure 1. *Photoisomerization of azobenzene. Adapted from* [3].

Azobenzene can be functionalized with different chemical moieties, allowing control over the spectroscopic properties of the material, for instance wavelength of excitation and stability of the *cis* isomer [12]. What is more, azobenzene and azobenzene derivatives can be incorporated into polymers and other compounds and fabricated into thin amorphous films [3].

Disperse Red 1 -glass, or DR1-glass in short, is a glass-forming compound derived from Disperse Red 1 (DR1) azo dye [13]. The molecular formula and typical absorption spectrum of the compound are presented in figure 2.
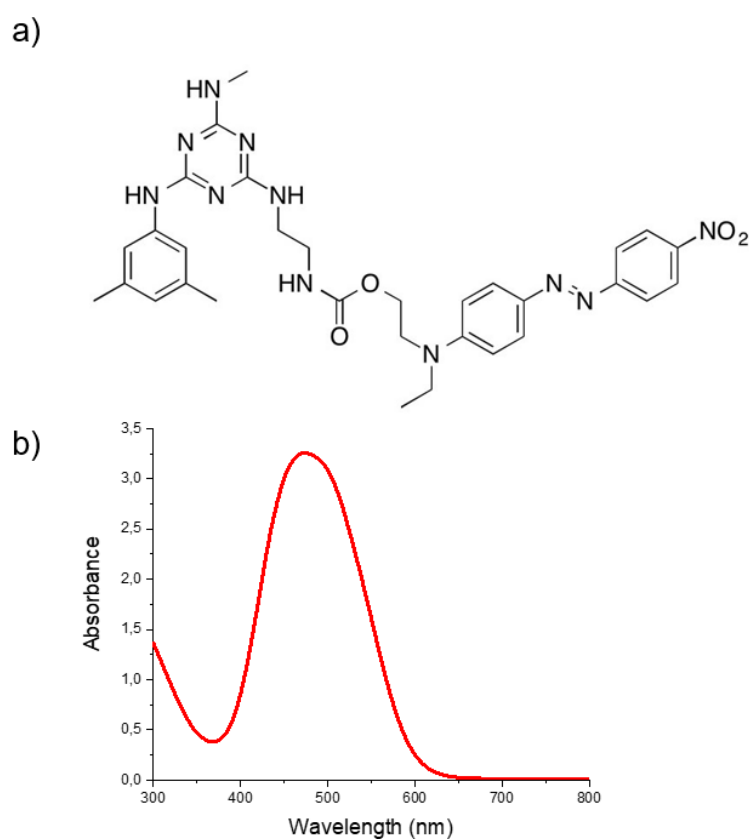
Figure 2. a) *The chemical structure of DR1-glass.* [13] **b)** *Absorption spectrum of a thin DR1-glass film spin coated from 9* mg/µl *DR1-glass solution in chloroform.*

In the DR1-glass, the mexylaminotriazine moiety promotes the formation of an amorphous film, whereas the Disperse Red 1 dye provides light-controllable properties to the films. [14]

DR1-glass films along with many other azobenzene containing films can be patterned by light-induced mass migration that results from the azobenzene photoisomerization. The

light induces continuous cycling between the two isomers, and this cycling is thought to trigger the mass migration process under, e.g., interference irradiation [10]. Sinusoidal patterns that are optically inscribed on the material upon irradiating the film with laser interference pattern, are called surface-relief gratings (SRGs), and these surface structures are formed when the material undergoes reorientation at molecular level as well as topographic rearrangement at the macroscopic level. [15] However, SRG formation is a highly complex process and the details of it are not yet perfectly understood. The topography of a typical SRG is presented in the atomic force microscopy (AFM) image shown in figure 3.
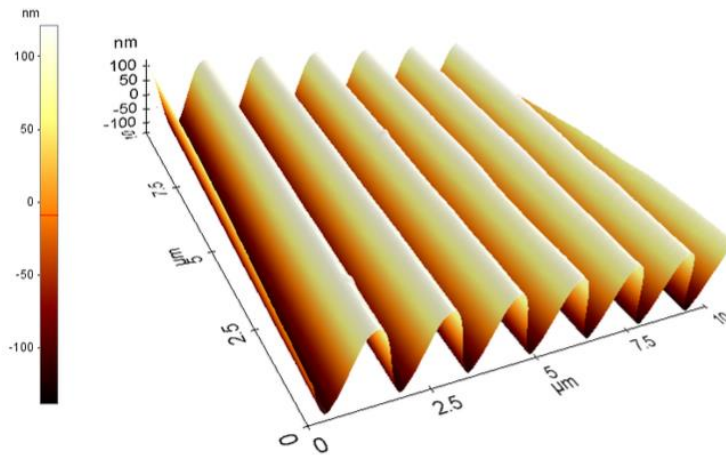

Figure 3. *AFM image of the surface topography on a DR1-glass film after SRG inscription.*

The surface-modulation depth of SRGs can be hundreds of nanometers, while the lateral period of the gratings can vary from few hundred nanometers up to several microns [10]. The SRGs can be inscribed, erased, and rewritten with light interference lithography [3]. Compared to common lithography techniques, such as electron beam lithography (EBL) and focused ion beam (FIB) lithography, the SRGs are extremely simple to fabricate, and provide beneficial features such as superposition of several SRGs and possibility to erase the structures, yet the spatial resolution obtained with EBL and FIB is much higher [16]. SRGs are utilized in many photonic applications, including holographic data storage as well as optical sensor and coupling devices [14]. In addition, controlling the material topography non-invasively and reversibly with light makes azobenzene compounds especially interesting for cell culturing applications and SRGs have been described to be able guide cell elongation and alignment along the surface topography [6].

2.2 Spin coating

Highly uniform, thin material coatings can be fabricated onto substrates utilizing various techniques, such as spin coating, dip coating and slot-die coating. Slot-die coating is an easily scalable technique, meanwhile the scalability of the other techniques is very limited. [17] Even so, spin coating is a simple and effective technique for fabricating thin, high-quality films for research purposes.

Spin coating is a technique used for depositing thin films of a material on flat substrates, such as glass coverslips or microscope slides, and for dispensing silicon wafers with photoresists in photolithography. During the procedure, the substrate is rotated at high speed, which causes the dispensed film solution to spread onto the substrate due to centrifugal forces, viscous forces, and surface tension of the solution. The film thickness can be varied from a few nanometers up to several microns. [9]

The spin coating process consists of dispensing, spinning (spin up and spin off), and evaporation. In the first step, the solution is pipetted or otherwise applied onto the substrate either dynamically or statically. [9] Dynamic dispensing means that the substrate is already spinning while the solution is added, while in static dispensing, the substrate is spun only after the dispensing. During the spinning, the solution spreads to the whole substrate and part of the solution is thrown from the substate, resulting in a thin, flat film. Finally, the solvent evaporates, leading to a thin, solid film. Figure 4 shows a schematic representation of the spin coating process.
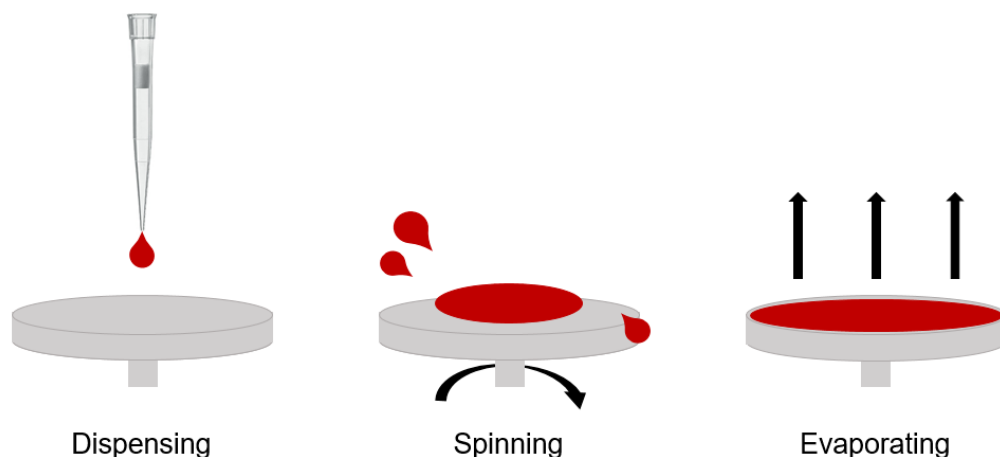

| Dispensing | Spinning | Evaporating |

Figure 4. *The spin coating process.*

The quality of the spin coated film is affected by material and solvent properties, but also by spin coating parameters and environmental factors, such as temperature and relative humidity [9]. The spin coating parameters that affect the quality of the sample are volume of the dispensed solution, dispensing style (dynamic or static), spinning speed as well as acceleration and spinning time.

The quality of spin-coated films can be verified by measuring the thickness of the films. Quality of the materials that absorb light in UV and visible region can also be verified by measuring the film absorption spectra. The dependency between absorbance and thickness can be expressed as

$$A(\lambda) = \alpha(\lambda)t,$$

(1)

where A is absorbance and α is the attenuation factor (nm^{-1}) at given wavelength, and t is thickness (nm). Therefore, the attenuation factor can be expressed as the relation between absorbance and thickness:

$$\alpha(\lambda) = \frac{A(\lambda)}{t}.$$

(2)

According to the literature, the thickness of a spin coated film is linearly dependent on the concentration of the solution used for spin coating [18].

$$t \propto ac,$$

(3)

where c is concentration (mg/μl) and a is the slope of the curve. Moreover, the thickness of a spin coated film is proportional to the inverse of the square root of the spinning speed [9].

$$t \propto \frac{1}{\sqrt{\omega}},$$

(4)

where ω is rotational speed (rpm). Functions 3 and 4 will later be utilized for fitting the dependency curves between the thickness and solution concentrations as well as the thickness and rpm values.

2.3 Optical setup for the SRG inscription

Lloyd's mirror setup can be utilized for SRG inscription of azobenzene-derived compounds fabricated into thin films. In the setup, half of the laser beam, also referred to as the writing beam, is reflected to the sample surface by a mirror at an angle. The reflected beam interferes with the beam directly impinging on the sample surface. When inscribing SRGs, a glass substate with light-responsive material film on top is placed on a sample holder and a writing beam with a proper wavelength is pointed to the sample. The light with such wavelength is absorbed by the film, and hence causing isomerization of the azobenzene units. The cyclic isomerization leads to mass migration, while the role of interference patterns is to create areas where the isomerization tendency differs [10]. Such differences are observed as formation of SRGs. The setup is presented in figure 5.
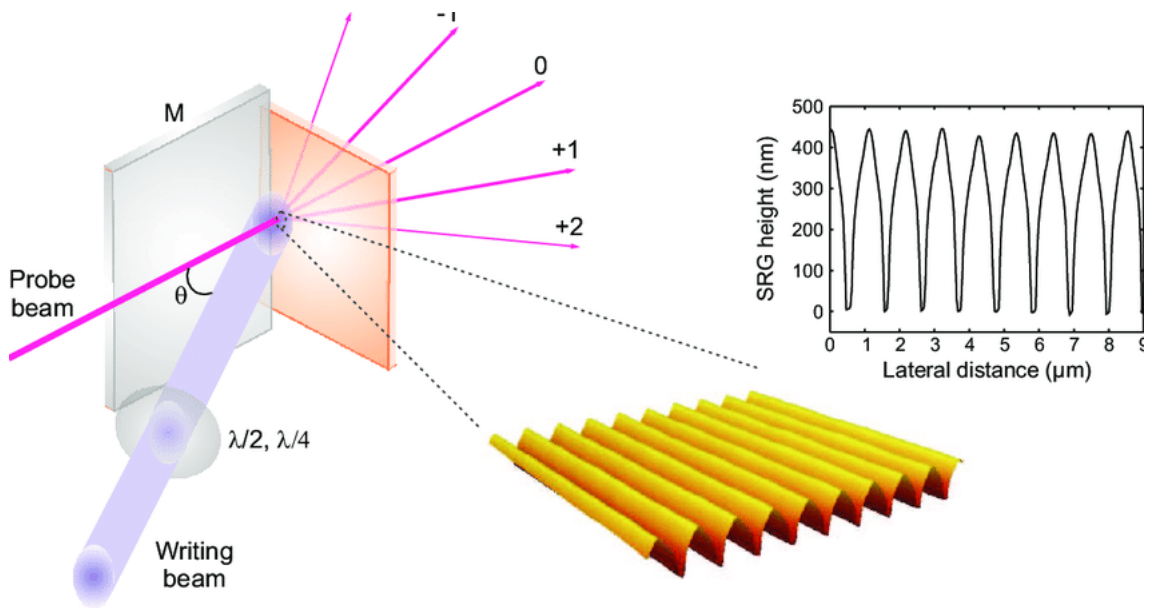
Figure 5. *A setup for the inscription of surface relief gratings. M refers to a mirror, λ/2 and λ/4 refer to waveplates used in polarization control of the beam. AFM micrograph of formed SRG and its typical profile are illustrated on the right.* [10]

The lateral period for the gratings is adjusted by changing the wavelength of the writing beam and the angle θ with which the beam hits the mirror [3].

$$\Lambda = \frac{\lambda}{2sin\theta},$$

(5)

where Λ is the lateral period (μm) and λ is the wavelength of the writing beam (nm). SRG surface-modulation depth is dependent on the material as well as the polarization and intensity of the writing beam and inscription time. [10]

A probe beam, for example a helium-neon (He-Ne) laser (633 nm), can be used to detect the formation of SRGs. When there are no SRGs, the probe beam goes straight through the sample without diffraction (figure 5, 0th-order beam). When the SRGs start to form, part of the probe beam is divided into the 1st-order, 2nd-order etc. diffracted beams shown in figure 5. As the SRG inscription proceeds, the intensity of the 0th-order beam decreases, whereas the intensity of higher-order diffracted beams increases up to a plateau. Thus, SRG formation can be monitored by measuring the power of the 1st-order diffracted beam.

Diffraction efficiency (DE) of the SRG can be expressed as the ratio between the power of the1st-order beam, P_1, and the power of the probe beam before the sample, P_0. DE is reported as a percentage between these two

$$DE = \frac{P_1}{P_0} \cdot 100 \text{ %}.$$

(6)

The DE values can be used for monitoring and comparing the SRGs of various samples. The topography and surface-modulation depth of the formed surface patterns can be observed and characterized for example with AFM or digital holographic microscopy (DHM).

2.4   Cytocompatibility of a material

The materials used in cell culture platforms need to be highly cytocompatible. Here, cytocompatibility means the property of a material not being harmful to the cells growing on the platform. In the natural tissue environment, cells may form junctions with one another and with the ECM, and these junctions take part in natural cell functions. Especially epithelial cells form both cell-cell and cell-ECM junctions to form a tight and polarized epithelium. [1] In addition, cell morphology is affected by many environmental factors and external signals. Hence, one way to study the cytocompatibility of a material is to evaluate the cell-cell and cell-material junctions along with cell morphology of the cells cultured on the material.

The morphology and junctions can be evaluated by observing certain biomarkers present in the cells. Actin is a multi-functional protein found in the cytoskeleton. It is involved in many cell functions, including cell division, cell signaling and maintenance of the cell

junctions. [19] E-cadherin is a transmembrane protein found in cell-cell junctions [20]. These junctions can be studied see if the epithelial cells form a tight, polarized epithelium. What is more, focal adhesion kinase (FAK) is a protein complex at the cell membrane that is present in the interface between cells and the ECM. Focal adhesions are involved in many cell functions, for example attachment and migration. [21] Phosphorylation of FAK indicates the formation of mature focal adhesions [3]. The aforementioned biomarkers will be later utilized in evaluation of the cytocompatibility of the platform.

2.5   Light-responsive cell culturing

As mentioned in the introduction, classic 2D cell culture platforms are poor in mimicking the natural microenvironment of cells, since they lack the dynamic characteristics of a tissue. Many cell functions are affected by the signals coming from the external environment of the cell, and without suitable stimuli, the cell phenotype can be altered or lost *in vitro* [3]. Consequently, smart biomaterials and stimuli-responsive cell culture platforms are essential for better mimicry of the natural, dynamic tissue.

Light-responsive materials, such as micelles, 2D surfaces and three-dimensional (3D) hydrogels have already been designed and applied in the research of various biological applications, including cell manipulation, cell encapsulation and controlled drug delivery [22]. For instance, Homma *et al.* have reported that the gene expression levels of E-cadherin can be controlled utilizing their azobenzene-bearing hydrogel [23]. On the other hand, Fedele *et al.* have presented the possibility of utilizing photopatterning of azopolymers in biomaterial surface modeling related to angiogenesis [24]. While there are still many challenges considering light-responsive cell culturing, these new smart materials and platforms are promising candidates for various biological and medical applications in the future.

Isomäki *et al.* utilize the photoisomerization of DR1–glass to affect and guide cell alignment. The material is photopatterned by interference lithography and Madin-Darby canine kidney type II (MDCK II) epithelial cells are cultured on top of the patterned film. They have reported that the SRG topography guides focal adhesion orientation along the surface topography even after the formation of uniform epithelial layer. In addition, the surface topography can be altered in the presence of live cells, enabling non-invasive control over the surface topography in real-time cell experiments. [3] Once the sample preparation protocol is optimized, this light-responsive cell culture platform could be used in research of complex cell-material interactions as well as cell behavior in dynamic environments.

3. RESEARCH METHODOLOGY AND MATE-RIALS

In this chapter, the experimental part of the thesis is described. The optimization phases are presented in sections 3.1 to 3.7. The sample quality was verified following 3.8 Quality assurance after each optimization phase. In addition, the cytocompatibility of the samples made with an optimized solvent mixture was tested as stated in section 3.9 Cell culture.

3.1 The starting point samples

The starting point samples were prepared following the protocol before optimization. DR1-glass (SOL80485, Solaris Chem Inc.) was dissolved in chloroform. 9 wt-% solution was spin coated on 22×22 mm glass coverslips which had first been ultrasonicated twice in acetone for 10 min. 35 µl of the DR1-glass solution was dynamically dispensed and spin coated at 1500 rpm for 35 s (spin coater, Laurell Technologies Corporation).

3.2 Solvent

The solvents for DR1-glass solution were chosen based on their chemical properties and previous experiences together with literature research of suitable solvents for spin coating. The used solvents and solvent mixtures were acetonitrile, chloroform, dichloromethane (DCM), dimethylformamide (DMF), ethanol, methanol, tetrahydrofuran (THF), toluene, 1,2-dichloroethane, chloroform-acetonitrile in 80:20 ratio (% v/v), chloroform-DMF in ratios of 60:40, 70:30 and 80:20 (% v/v), chloroform-methanol in 80:20 ratio (% v/v), chloroform-toluene in 10:1 ratio (% v/v) and chloroform-1,2-dichloroethane in ratios of 1:1 and 80:20 (% v/v).

The samples were spin coated similarly to the starting point samples. After spin coating, the samples were kept in a vacuum chamber at 60 °C for 60 min to ensure that the solvents had fully evaporated from the films. Heat treatment in the vacuum chamber was repeated in all the following phases of the optimization.

3.3 Preparation of the spin coating solution

Slight modifications for the preparation of the spin coating solution were made to improve the homogeneity of the samples. First, the solution was ultrasonicated at 45 °C temperature for 2 min to help material dissolution.

After sonication, the solution was let to cool down to room temperature and filtered with 0,2 μm PTFE filter with a diameter of 13 mm. Following the filtration, the solution was ultrasonicated again at 45 °C for 2 min. The solution was let to cool down to room temperature before spin coating to prevent the solvent from evaporating too fast. These modifications were used for all the phases described onwards.

3.4   Spin coating parameters

Optimal spin coating parameters were searched by systematically changing one variable at a time and checking the film quality between each parameter change. When using dynamic dispensing and a solvent that evaporates extremely fast, the volume of a dispensed solution and spinning speed are the parameters that have a major effect on the quality of a sample. The solutions were prepared as stated earlier.

First, a suitable amount of a solution was found by spin coating various volumes using dynamic dispensing at 1500 rpm. Volumes were tested every 5 μl between 30 and 60 μl. After an optimal volume was found, a spinning speed was screened changing speeds every 250 rpm between 1000 and 3000 rpm.

3.4.1   Concentration-rpm series

A concentration series of DR1-glass solutions was prepared by dissolving DR1-glass in chloroform-1,2-dichloroethane (80:20 % v/v) in concentrations of 3 wt-%; 4,5 wt-%; 6 wt-%; 7,5 wt-% and 9 wt-%. 35 μl of the DR1-glass solutions were dynamically spin coated on microscope slides (25×25 mm) that had first been ultrasonicated in acetone for 20 min. Used rpm values were 1000, 2000 and 3000.

The film quality was verified, and the thickness of the samples was measured with a profilometer (DEKTAK-150 STYLUS Profiler, Veeco) using 6,5 μm measurement range, 2,5 μm range and 0,022 μm resolution. Thickness measurements were performed twice on 3 wt-%, 6 wt- % and 9 wt-% samples and once on the rest. The thickness values for 3 wt-%, 6 wt-% and 9 wt-% samples are presented as average values.

3.5   Glass substrate cleaning methods

Various methods for cleaning the glass substrate were tested to see if cleaning affects the quality and reproducibility of the films prepared by spin coating. Coverslips were cleaned by ultrasonicating them with diverse solvent combinations. The tested solvents

and combinations were acetone 10 min, acetone 2×10 min, isopropanol 10 min, isopropanol 2×10 min, acetone 10 min followed by isopropanol 10 min, and isopropanol 10 min followed by acetone 10 min.

Moreover, the effect of oxygen plasma treatment on the coverslips was tested. Here, the substrates were first ultrasonicated twice in acetone for 10 min and then plasma treated for 2 min with high plasma power (Plasma cleaner and Plasmaflo PDC-FMG, Harrick Plasma).

6 wt-% DR1-glass solution was prepared as stated earlier. The solution was spin coated on the substrates cleaned with the aforesaid methods.

3.6   SRG inscription

6 wt-% DR1-glass samples were prepared for analyzing the final effect of the optimization. The detailed sample preparation protocol is presented in attachment 1 - Optimized preparation protocol for thin DR1-glass films.

The SRG inscription was performed using a 488 nm continuous-wave laser (Genesis CX488-2000, Coherent) with circular polarization. The microtopography period was set to 2 µm and intensity to 500 mW/cm^2 over the half-circular 0,25 cm^2 area. After inscription, a 633 nm He-Ne laser was used for measuring the 1st-order beam powers at 10 spots on each SRG (LabMax-TO laser power meter, Coherent). Measured maximum values were then used for defining the final diffraction efficiencies of the SRGs. The inscription was performed on four different samples and twice on one of the samples, five times in total. Moreover, the SRG formation on the samples was verified by DHM (DHM R2104, Lyncée Tec).

3.7   User dependency

Finally, the optimized sample preparation protocol for DR1-glass thin films was tested by four different users. Each of the four prepared 6 wt-% DR1-glass solution enough for five samples. The samples were prepared following the optimized protocol presented in attachment 1. The data from the quality assurance was used for examining user-dependent differences in sample preparation.

3.8   Quality assurance

Samples were imaged with a polarized optical microscope (Zeiss Axio Scope.A1, N-Achroplan air-immersion 5×/0,13 Pol ∞/0 objective). Additionally, absorbances of the

samples were measured between wavelengths from 300 nm to 800 nm with a UV-vis spectrophotometer (Cary 60 UV-vis, Agilent Technologies). The absorption spectra were plotted on averaged data of a varying number of samples and measuring spots per sample. The number of samples and measuring spots that were used for the absorption measurements are presented in table 1.

Table 1. *The numbers of samples and measuring spots for absorbance curves in different optimization phases.*

Phase	Number of samples per sample type	Number of measuring spots per sample
3.1 The starting point samples	3	5
3.2 Solvent	3	5
3.4 Spin coating parameters	2	5
3.4.1 Concentration-rpm series	2	5
3.5 Glass substrate	2	5
3.6 SRG inscription	10	3
3.7 User dependency	3	5

The samples from phases 3.1, 3.6 and 3.7 were imaged a digital single-lens reflex camera (CANON EOS 1100D, EFS 18-55 mm MACRO 0,23/0,8ft lens) to demonstrate the differences in the appearance quality of the samples. The data from the quality assurance of the optimization process is presented in Chapter 4. Results and discussion.

3.9 Cell culture

Cytocompatibility of the samples made with an optimized solvent mixture was tested by culturing MDCK II cells on top of the DR1-glass films. The solvent mixture was chosen based on the experiments described in Section 3.2.

9 wt-% DR1-glass samples were prepared in chloroform-1,2-dichloroethane in 80:20 ratio (% v/v), while ultrasonicated coverslips were used as control samples. Before cell seeding, the samples were coated with 50 µg/ml monomeric rat tail type I collagen solution (Thermo Fischer Scientific) in 0.02 N acetic acid and sterilized under UV light for 40 min. MDCK II cells were seeded and cultured on top of the samples for 72 hours.

After 72 hours of the cell seeding, the cells were fixed with 4 % paraformaldehyde (PFA) and rinsed twice with 1,5 ml of PBS. 2 ml of PBS was added to the wells and the samples were stored at +4 °C overnight.

The samples were first immunolabeled with primary antibodies. PBS was aspirated from the wells and 1 ml of permeabilization buffer, containing 0,5 % Bovine serum albumin (BSA) (PAN Biotech) and 0,5% Triton X-100 (Sigma-Aldrich) in PBS was added and incubated in room temperature for 10 min. The buffer was aspirated and 1 ml of 3 % BSA in PBS was added and incubated at room temperature for 1 hour. The samples were gently dried and 100 µl of 1:200 solution of rabbit anti-pFAK (Sigma Alrich) in 3 % BSA was added on top of the samples. The samples were incubated at room temperature for 1 hour.

The solution was aspirated, and samples washed with 1,5 ml of PBS for 10 min. The samples were then gently dried and 100 µl of 1:100 solution of rat anti-Uvomorulin/E-cadherin (Invitrogen) in 3 % BSA was added. The well plates were sealed with parafilm and incubated at + 4 °C until the next day.

In the following day, the samples were immunolabeled with secondary antibodies. The samples were first washed 3 times with 1,5 ml of PBS for 10 min. After, 100 µl of the antibody solution was added, containing 1:200 A647 anti-rabbit-Alexa (Thermo Fisher Scientific), 1:200 A568 anti-rat-Alexa (Thermo Fisher Scientific) and 1:50 Atto 488-Phalloidin (Sigma-Aldrich) in 3 % BSA. The samples were incubated covered from light at room temperature for 1 hour. Next, the samples were washed twice with 3 ml of PBS for 10 min and with 2 ml of MilliQ water. After washing, the samples were immediately mounted on top of microscope slides, using Prolong Diamond Antifade Mountant with 4',6'diamidino-2-phenylindole (DAPI) (Invitrogen). The samples were dried covered from light at room temperature overnight.

Mounted samples were imaged with a confocal microscope (Nikon A1R laser scanning confocal microscope) using 405 nm, 488 nm, 561 nm, and 633 nm laser lines. 60×/1,4 Plan-Apochromat oil immersion DIC N2 objective was used to capture 1024×1024-pixel 3D z-stack images that were used for evaluating cell morphology.

4. RESULTS AND DISCUSSION

In this chapter, the results of the experiments are presented. In addition, the causal connections and considerations of the results are also discussed. The chapter is divided into five separate sections: 4.1 The starting point samples, 4.3 Solvent, 4.3 Spin coating parameters, 4.4 User dependency and other error sources and 4.5 Cell culture.

4.1 The starting point samples

9 wt-% DR1-glass samples were spin coated in chloroform. The samples were imaged with a polarized optical microscope and a digital single-lens camera. Images representing the average quality of the sample population are shown in figure 6.
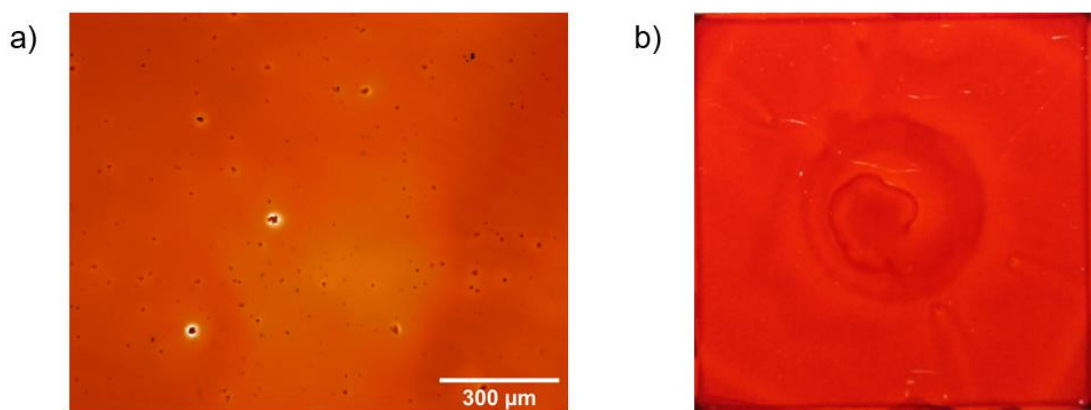

Figure 6. *The average quality of the population of the starting point samples.* **a)** *9 wt-% DR1-glass film imaged with a microscope, scale bar: 300 µm.* **b)** *9 wt-% DR1-glass film imaged with a digital single-lens camera. Sample size: 22×22 mm.*

The dark spots in the microscope image are solid aggregates of DR1-glass and possible material splashes from dispensing the material onto the substrate. In addition, the film thickness is varying from area to area, which can be seen as changes in the color intensity on the samples. The color changes and material swirls are also visible to the naked eye. The darker circle in the middle of the sample originates from the vacuum of the spin coater – The vacuum that holds the substrate still while spin coating bends the cover slip slightly, causing the middle part to be a bit thicker than the rest of the film.

Absorbances of three separate samples and five spots each were measured with a UV-vis spectrophotometer to observe the film differences in more detail. The averaged absorption spectra of all the measured absorbances are presented in figure 7 together with the standard deviation. In addition, the absorbance differences of 5 separate measuring spots inside one sample as well as the differences between three samples are illustrated.
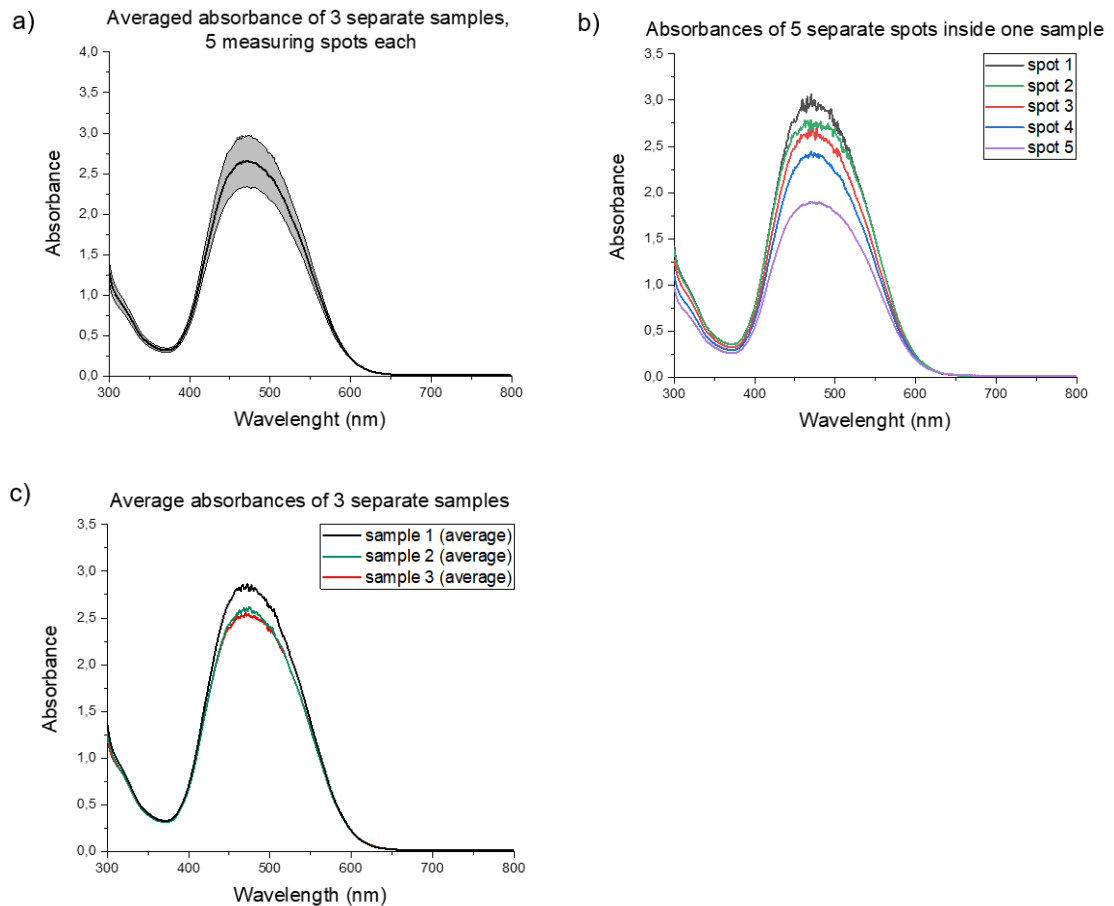

Figure 7. *The starting point samples.* **a)** *An average absorption spectrum and standard deviation.* **b)** *Absorption spectra of five measuring points inside one sample.* **c)** *Average absorption spectra of three separate samples. Here, each curve is averaged from five measuring spots.*

Figure 7 confirms that the deviation of the sample thickness and absorbance is prominent. There are major differences in point-to-point absorbance curves measured inside a single sample, meanwhile the sample-to-sample differences in averaged absorbances are smaller. Therefore, the inhomogeneity of the DR1-glass film is the largest cause of variation in the samples.

4.2   Solvent

One of the reasons for the non-uniformity of the samples is the solvent used in sample preparation. Chloroform is an extremely volatile solvent leading to very fast drying of the film when spin coating. Rapid evaporation causes uneven areas in the film and the swirls of material can be seen on the film, because the material has begun to dry when still dispensing the material. One way to improve the uniformity of the film is to use a less volatile solvent [9]. Now, various solvents were tested.

Another way to improve the uniformity of the spin coated film is to use a solvent blend instead of only using one solvent. A major component of a solvent that evaporates quickly and a minor component of another solvent that evaporates in a slower fashion are mixed. The minor component slows down the drying of the film and there's more time for the molecules to organize on a substrate resulting in more uniform and higher quality films. [9] Now, chloroform was mixed with a few solvents in different ratios to test if solvent blends work better for spin coating than using pure solvents. The solvents and solvent blends tested are presented in the table 2.

Table 2. *Tested solvents and solvent blends along with the appearances of the spin coated DR1-glass films.*

	Solubility of DR1-glass (S=soluble, I=insoluble)	Microscopy	Film appearance	Filtration
Acetonitrile	I	No	-	No
Chloroform	S	Yes	Moderate	Yes
DCM	S	Yes	Lousy	No
DMF	S	Yes	Lousy	No
Ethanol	I	No	-	No
Methanol	I	No	-	No
THF	S	Yes	Good	No
Toluene	I	No	-	No
1,2-dichloro-ethane	S	Yes	Good	Yes
Chloroform-acetonitrile (80:20)	S	Yes	Lousy	No
Chloroform-DMF (60:40)	S	Yes	Lousy	No
Chloroform-DMF (70:30)	S	Yes	Lousy	No
Chloroform-DMF (80:20)	S	Yes	Lousy	No
Chloroform-methanol (80:20)	S	Yes	Lousy	No
Chloroform-toluene (10:1)	S	Yes	Lousy	No
Chloroform-1,2-dichloro-ethane (80:20)	S	Yes	Excellent	Yes

Based on microscope imaging, the best quality films are accomplished when using a blend of chloroform and 1,2-dichloroethane in 80:20 (% v/v) ratio. The data is presented in figure 8.
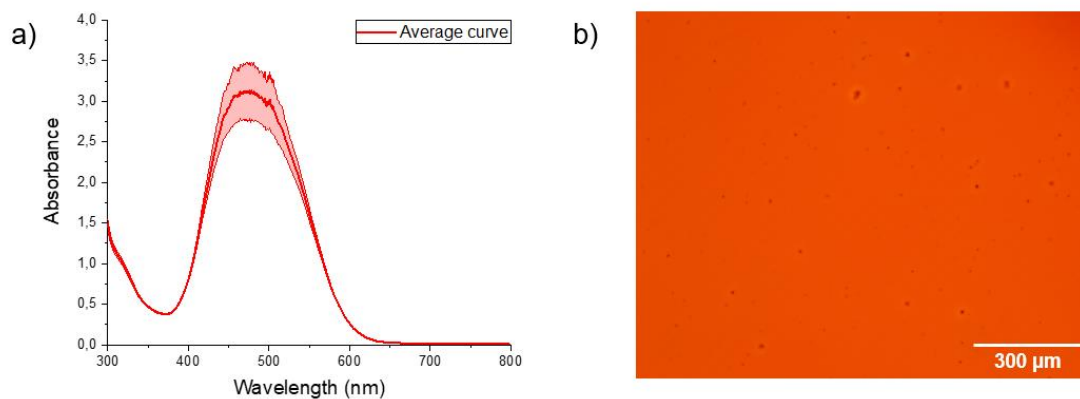
Figure 8. *9 wt-% DR1-glass film in chloroform-1,2-dichloroethane (80:20 % v/v).* **a***) An average absorption spectrum and standard deviation.* **b)** *A microscope image of a film, scale bar: 300 μm.*

Here, there is no major improvement in the absorption spectra of the samples prepared in chloroform-1,2-dichloroethane blend compared to using pure chloroform. Still, the material swirls on the films could no longer be seen, and the overall appearance of the film is notably better than with bare chloroform or other tested solvents or solvent blends. In other words, the change of the solvent considerably improves the quality of DR1-glass films.

Since the deviation of the absorbance was still large after changing the solvent, filtration of the solution was added to the film preparation protocol to reduce the DR1-glass aggregates on the films. PTFE filters with a 0,2 μm pore size were used for this purpose. In addition, the solution was ultrasonicated before and after filtration to agitate the solution and consequently improve the solubility of DR1-glass and dissipate material aggregates into smaller pieces. The samples were imaged with a polarized optical microscope and the absorption spectra was measured with a UV-vis spectrophotometer. The data is shown in figure 9.
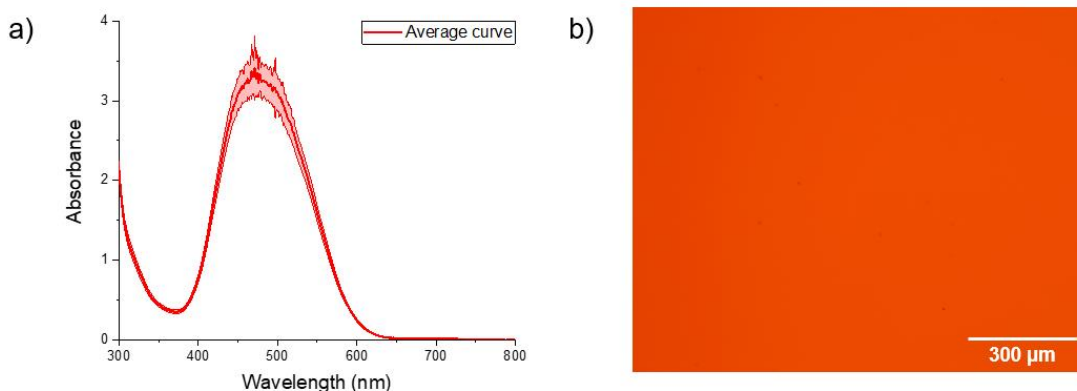
Figure 9. *9 wt-% DR1-glass in chloroform-1,2-dichloroethane (80:20 % v/v), filtered solution.* **a)** *An average absorption spectrum and standard deviation.* **b)** *A microscope image, scale bar: 300 µm.*

The films prepared with a filtered solution contain notably less aggregates than films prepared without filtration. The number of aggregates were manually calculated from three microscope images of the films before and after filtration to estimate the effect of filtration quantitatively. The microscope images before filtration contain an average of 161 aggregates, whereas the corresponding number after filtration is 58. Thus, the number of aggregates was decreased by 70 %. It is also evident by eyes that the aggregate size in filtrated samples is much smaller than in non-filtrated samples. Moreover, filtration decreases the standard deviation of the absorption spectra of the samples. Hence, filtration together with sonication of the solution improves the quality and reproducibility of the DR1-glass samples.
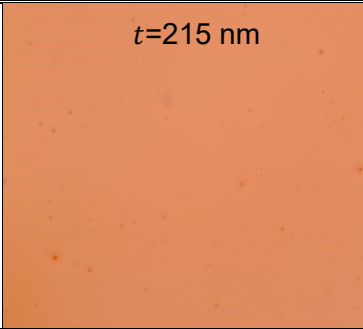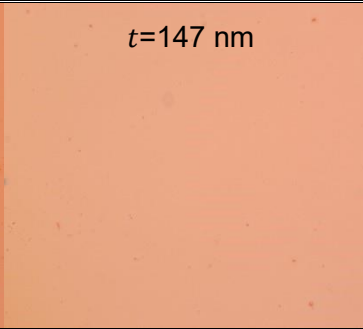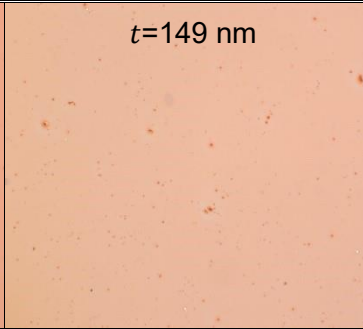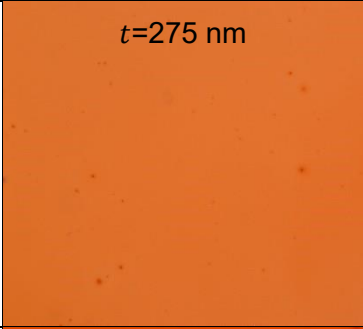
4.3   Spin coating parameters
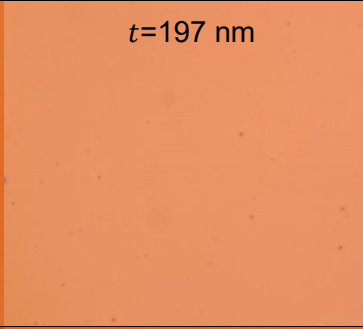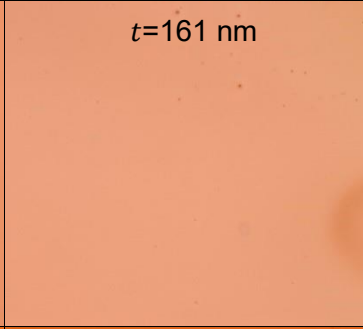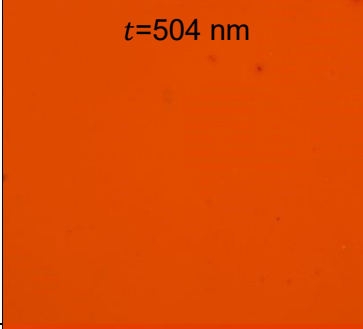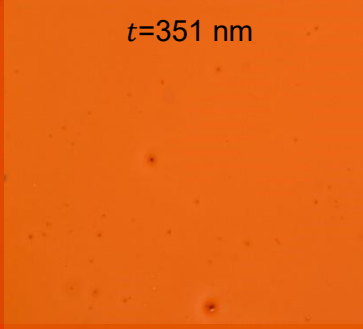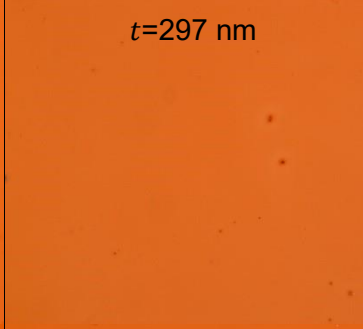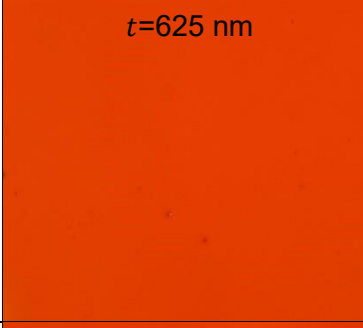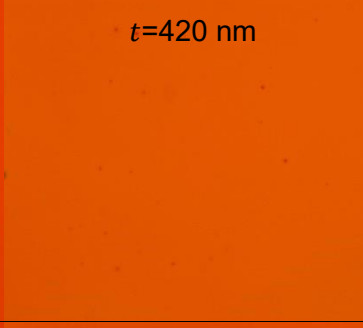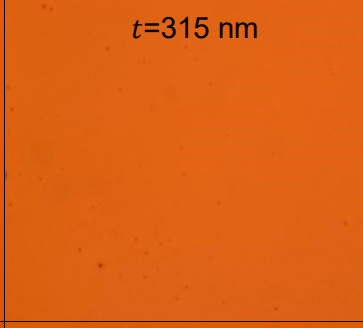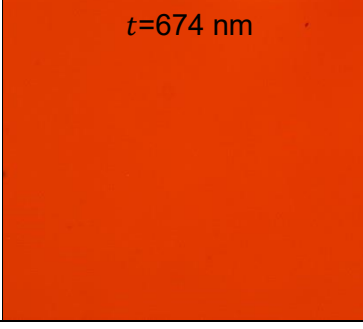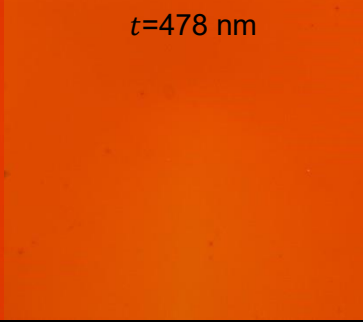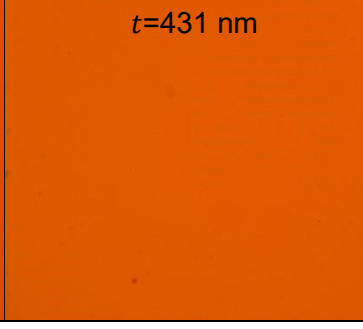
Optimal spin coating parameters were searched by systematically changing one parameter at a time and comparing the overall appearances of the samples as well as comparing the absorbances of the films. The best results were obtained with a volume of 35 µl and rpm of 3000. Increasing the spinning time and acceleration did not affect the quality of the film, since the DR1-glass film dried almost completely during 35 seconds of spinning and the substrate was already spinning in full speed when the solution was dynamically dispensed.

Use of static dispensing produces thicker films than use of dynamic dispensing. Now, there was no need to prepare thicker films, and therefore static dispensing was not widely

researched. Besides, literature suggests that using dynamic dispensing compared to static one can improve the repeatability and quality of the film [25].

Concentration of the solution and rotational speed both affect the thickness of the film prepared by spin coating. A concentration-rpm sample series were prepared by spin coating samples with a concentration from 3 wt-% to 9 wt-% every 1,5 wt-% using rotational speeds of 1000, 2000 and 3000 rpm. The samples were imaged with a polarized optical microscope and the absorbances were measured with a UV-vis spectrophotometer. In addition, the thickness values of the samples were measured with a profilometer. Thicknesses of 3 wt-%, 6 wt-% and 9 wt-% samples were measured twice, and values were averaged, while other concentrations were only measured once. A matrix of the microscope images and measured thickness values are presented in table 3.

Table 3. *Concentration-rpm series of DR1-glass: Microscope images and thickness values measured with a profilometer.*

wt -%	1000 rpm	2000 rpm	3000 rpm
3	t=215 nm	t=147 nm	t=149 nm
4,5	t=275 nm	t=197 nm	t=161 nm
6	t=504 nm	t=351 nm	t=297 nm
7,5	t=625 nm	t=420 nm	t=315 nm
9	t=674 nm	t=478 nm	t=431 nm

The variation in film thickness is visible when comparing the colors of the spin coated films – The darker the color, the thicker the film. Thus, the film prepared with a 3 wt-% solution with rpm value of 3000 is the thinnest one, meanwhile the film prepared with a 9 wt-% solution with rpm value of 1000 is the thickest one. Now, the measured thickness for 3 wt-% DR1-glass spin coated at 3000 rpm was a bit higher than for the same concentration spin coated at 2000 rpm, which probably originates from small locational differences in the thicknesses of the films. The profilometer is a precise instrument, but it only measures a very small area on a sample, and therefore, locational differences strongly affect the results of thickness measurements.

Absorbances of the samples were measured from two replicate samples, 5 measuring spots each. Absorbance values $A(\lambda)$ were averaged for each sample type. The thickness values along with maximum absorbances are shown in table 4.

Table 4. *Thickness values and maximum absorbances of DR1-glass concentration-rpm series.*

Sample	1000 rpm		2000 rpm		3000 rpm	
	t (nm)	$A(\lambda)$	t (nm)	$A(\lambda)$	t (nm)	$A(\lambda)$
3 wt-%	215	1,07	147	0,79	149	0,67
4,5 wt-%	275	1,47	197	1,02	161	0,86
6 wt-%	504	2,65	351	2,22	297	1,78
7,5 wt-%	625	3,36	420	2,23	315	1,85
9 wt-%	674	5,72	478	2,57	431	2,27

Knowing the attenuation factor, it is possible to estimate the film thickness, once $A(\lambda)$ is known. The attenuation factors were calculated using equation 2 for each sample in the concentration-rpm series. Based on these calculations, the averaged attenuation factor for thin DR1-glass films is $\alpha_{av} = 0,0056$ nm^{-1} with a standard deviation of $0,0009$ nm^{-1}. Thus, the average dependency between film thickness and absorbance is approximately $\alpha_{av} = 0,0056 \pm 0,0009$ nm^{-1}. The deviation is mainly caused by measuring errors of absorbance values of the samples that were ultimately thick or thin due to inaccuracy of the spectrophotometer on such values. In addition, the small locational differences of the thicknesses of the films once again affect the values measured with a profilometer and therefore affect the averaged attenuation factor.

As stated above, the calculated average attenuation factor can be used for estimating film thicknesses. For example, the measured maximum absorbance value for 4,5 wt-%

DR1-glass with rotational speed of 3000 rpm is $A(4{,}5\,wt-\%, 3000\,rpm) = 0{,}86$. Therefore, an estimation for the film thickness is

$$t_{estimate}(4{,}5\text{ wt}-\%, 3000rpm) = \frac{A(4{,}5\text{ wt}-\%, 3000\,rpm)}{\alpha_{av}} = \frac{0{,}86}{0{,}0056\,nm^{-1}} = 153{,}57142\ldots\text{nm} \approx$$

154 nm, while the measured thickness is $t_{measurement}(4{,}5\text{ wt}-\%, 3000\,rpm) = 161$ nm. The difference between the estimated and measured values is reasonably small and therefore the averaged attenuation factor is a functional way of estimating DR1-glass film thicknesses without profilometry.

As stated in Section 2.3, according to the theory of spin coating, the thickness of a spin coated film is linearly dependent on the concentration of the dispensed solution and proportional to the inverse of the square root of the spinning speed [18, 9]. Here, the concentration has a bigger impact on the film thickness, while the rotational speed values can be used for fine tuning. The concentrations and thickness measurement results were plotted and fitted with equation 3. Similarly, the rotational speed values and the thickness measurement results were plotted and fitted with equation 4. The graphs are presented in figure 10.
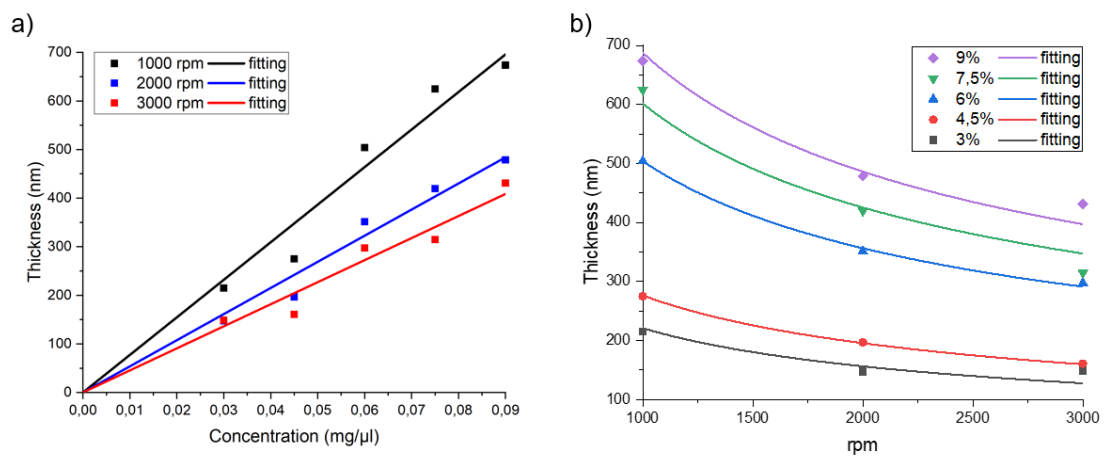
Figure 10. a) *The thickness-concentration dependency of spin coated DR1-glass films. The fitting is in form $y = ax$, where y is the thickness (nm), x is the concentration in* mg/µl *and parameter a is the slope of the curve.* **b)** *The thickness-rpm dependency of spin coated DR1-glass films. The fitting is in form $y = b\frac{1}{\sqrt{x}}$, where y is the thickness (nm), x is the rpm value and parameter b is a coefficient. The parameters were calculated via Origin Graphing & Analyses program (Origin, v. 2019b, OriginLab Corporation).*

In figure 10a, the measured points are well positioned in respect to the fitted lines, ergo, the dependency between the concentration and thickness is linear. Here, the best correspondence between the points and the fit is obtained at 3000 rpm, which is explained by the fact that the best-quality films were obtained at that value.

Respectively, in figure 10b, the measured points are positioned in respect to the fittings and therefore, the thickness of a spin coated DR1-glass film is indeed proportional to the inverse of the square root of the spinning speed. 4,5 wt-% and 6 wt-% samples are positioned to the fits especially well, while the measured points of the highest and lowest concentrations differ from the fits slightly more. The differences are mainly caused by measuring errors due to inaccuracies of the spectrophotometer on such values.

Figure 10 enables choosing a suitable concentration and rotational speed for spin coating when a certain film thickness is needed. For instance, if the needed thickness is 400 nm, each graph offers three alternatives for concentration and rotational speed that can be used to prepare such films as visualized in figure 11.
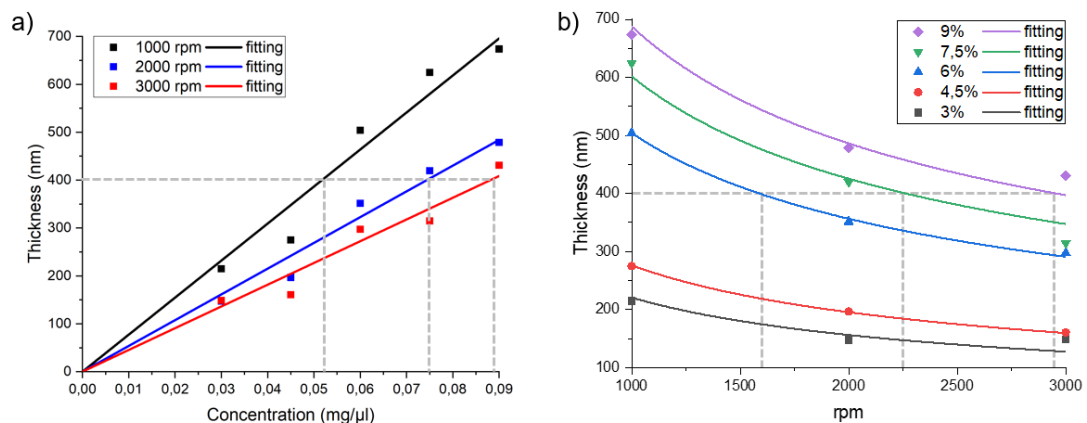
Figure 11. *Representation how to use the graphs for finding concentrations and rpm values for the preparation of 400 nm thick DR1-glass films.* **a)** *Concentrations based on the thickness and rpm-values.* **b)** *Rpm-values based on the thickness and concentration.*

Looking at figure 11a, the options for preparing 400 nm thick films are 5,2 wt-% DR1-glass spin coated at 1000 rpm, 7,5 wt-% DR1-glass spin coated at 2000 rpm and 8,9% DR1-glass spin coated at 3000 rpm. In figure 11b, the options for preparing 400-nm thick films are 6 wt-% DR1-glass spin coated at 1600 rpm, 7,5 wt-% DR1-glass spin coated at 2250 rpm and 9 wt-% DR1-glass spin coated at 2950 rpm. Despite the values are only

indicative, the graphs offer a valuable tool for finding proper parameters for light-responsive cell culturing along with other potential uses of thin DR1-glass films.

After other parameters were optimized, a few different cleaning methods for glass substrates were tested to see whether the methods affect the films. Usage of acetone and isopropanol alone and their usage one after another was tested when ultrasonicating the substrates. In addition, oxygen plasma treatment as a cleaning method before spin coating was tested.

The results for testing glass substrate cleaning methods reveal that there are no major differences between films that were spin coated on cover slips cleaned with diverse methods. Still, even if the differences are negligible, the films that were spin coated on cover slips that had first been ultrasonicated in isopropanol for 10 minutes and then in acetone for 10 minutes, have the smallest standard deviation in the absorption spectrum. Consequently, ultrasonication in isopropanol and acetone was added to the optimized preparation protocol.

The improvement of the film appearance, uniformity and reproducibility during the optimization process was indicated by spin coating 10 samples with the optimized protocol. The quality check for the sample population was performed by imaging the samples with a polarized optical microscope and a digital single-lens camera, and by measuring the absorption spectra between 300 and 800 nm. The comparison between the starting point samples and the samples made with the optimized protocol is presented in figure 12.
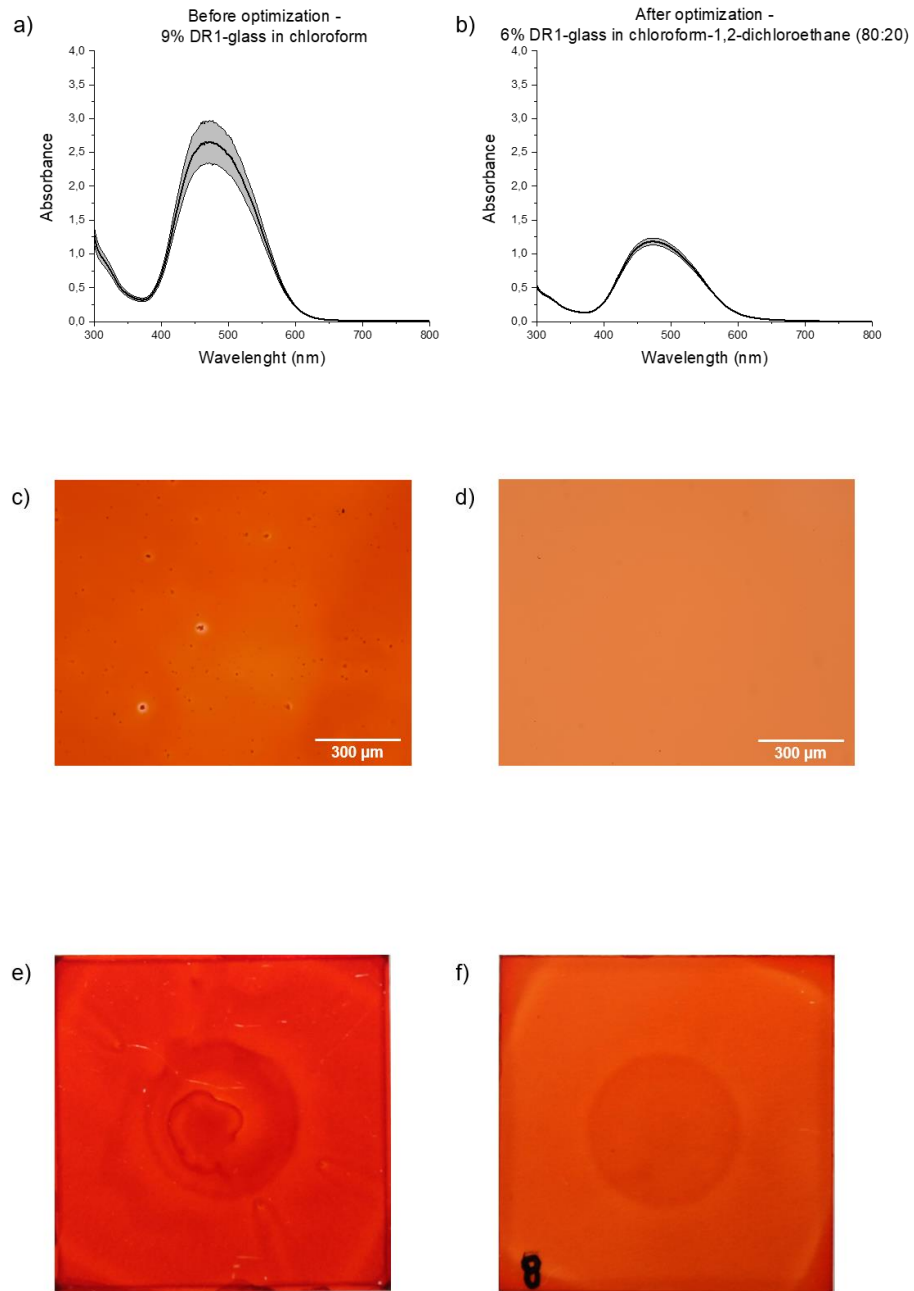
Figure 12. *DR1-glass samples before and after optimization. The data represents the quality of the average samples.* **a)** *The average absorption spectrum of 9 wt-% DR1-glass before optimization (3 samples, 5 measuring spots each).* **b)** *The average absorption spectrum of 6 wt-% DR1-glass after optimization (10 samples, 5 measuring spots each).* **c)** *A microscope image before optimization, scale bar: 300 μm.* **d)** *A microscope image after optimization, scale bar: 300 μm.* **e)** *A sample before optimization imaged with a single-lens camera. Sample size: 22×22 mm.* **f)** *A sample after optimization imaged with a single-lens camera. Sample size: 22×22 mm.*

Based on the results, the deviation in the absorption spectra decreased considerably during the optimization. The maximum standard error in the absorption spectra before optimization is 0,084, meanwhile the corresponding value after optimization is 0,007. In other words, the maximum standard error was decreased by over 90 %. The differences in the maximum absorbance values and sample color intensities in figure 12 originate from decrease in concentration and increase in rotational speed of spin coating.

Overall, the film appearance is massively improved. The microscope images show that samples made with the optimized protocols are uniform and no longer contain large material aggregates. In addition, visible material swirls have been eliminated by the optimization.

The darker circle in the middle of the samples still originates from the vacuum of the spin coater, but this issue could be solved by using a vacuum-free spin coating adapter [9]. Another way to eliminate the effect of the vacuum is to use thicker glass substrates, for example microscope slides. The very corners of the sample are a bit darker and thicker than the rest of the film, since material is moving from the center of the sample to the sides while spinning, and therefore more material is drying onto the corners. Regardless, the uniform area of the sample is large enough for using the samples in light-responsive cell culturing.

Finally, SRG inscription was performed five times in total, on four optimized samples, to compare the samples to one another, and to show the light-responsive property of the films. The inscription was performed with an intensity of 500 mW/cm^2 and a circular polarization for 10 minutes. After inscription, the 1st-order beams were measured with a 633 nm He-Ne laser and the maximum values were used for calculating the diffraction efficiencies using equation 6. The calculated values are presented in table 5.

Table 5. *Diffraction efficiency values of optimized DR1-glass samples*.

Sample	DE (%)
1	12
2	13
3	14
4, SRG 1	13
4, SRG 2	14

Before optimization, Isomäki *et al.* have reported the standard deviation for the final DE values of DR1-glass to be ±7 % [3]. Similarly, Lim *et al.* have inscribed SRGs on thin poly(disperse red 1 methacrylate) films with holographic inscription, and they illustrate the error of the DE values to be around 7 % [26]. Now, the average DE value for optimized 6 wt-% DR1-glass samples is 13,20 % whereas the standard deviation is 0,84 %. Therefore, the standard deviation value has considerably decreased during optimization. The standard deviation of DE is also considerably smaller for SRGs inscribed on optimized DR1-glass compared to previously reported values.

Along with the DE measurements, the SRG formation was confirmed by profiling the SRG topography with DHM. The data is presented in figure 13.
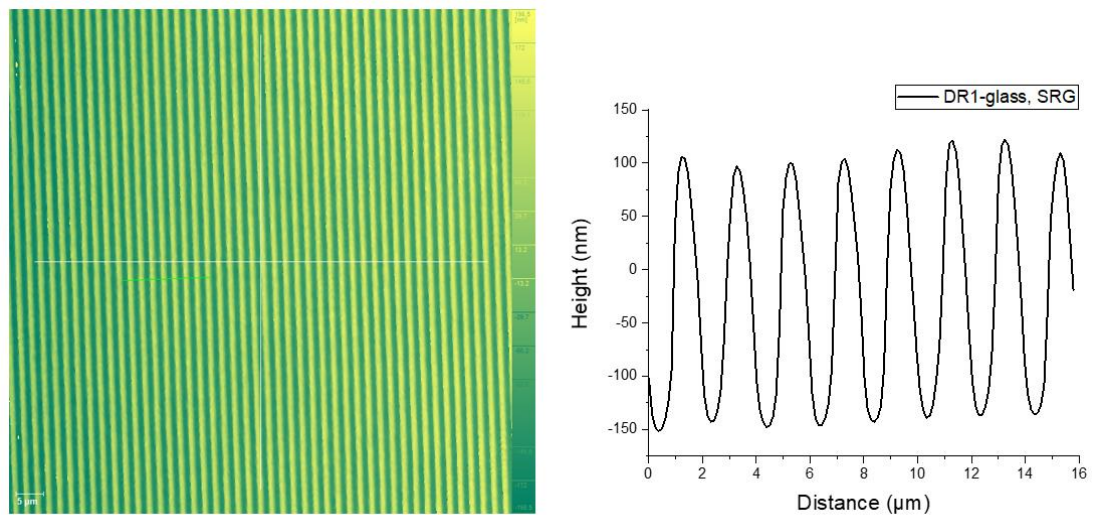
Figure 13. *DHM image and profile of SRG topography on a 6 wt-% DR1-glass film spin coated at 3000 rpm.*

Figure 13 confirms that the SRGs are formed and that the gratings are regular and homogeneous inside the patterned area. Additionally, the patterns of separate samples resemble one another. In conclusion, the DE values along with DHM profiling indicate that the optimized samples are homogenous enough to provide data with a reasonable error for advanced light-responsive cell culturing.

4.4   User dependency and other error sources

The user dependency on the film quality was tested by having 4 different users prepare 5 samples following the new, optimized protocol. The samples were imaged with a polarized optical microscope and a single-lens camera. Three best samples of each user were used for absorbance measurements. The data of the samples made by the four users (B-E) is presented in the next page together with data from the thesis author's samples (A) (figure 14).

a)
User A

b)
User B

c)
User C

d)
User D

e)
User E

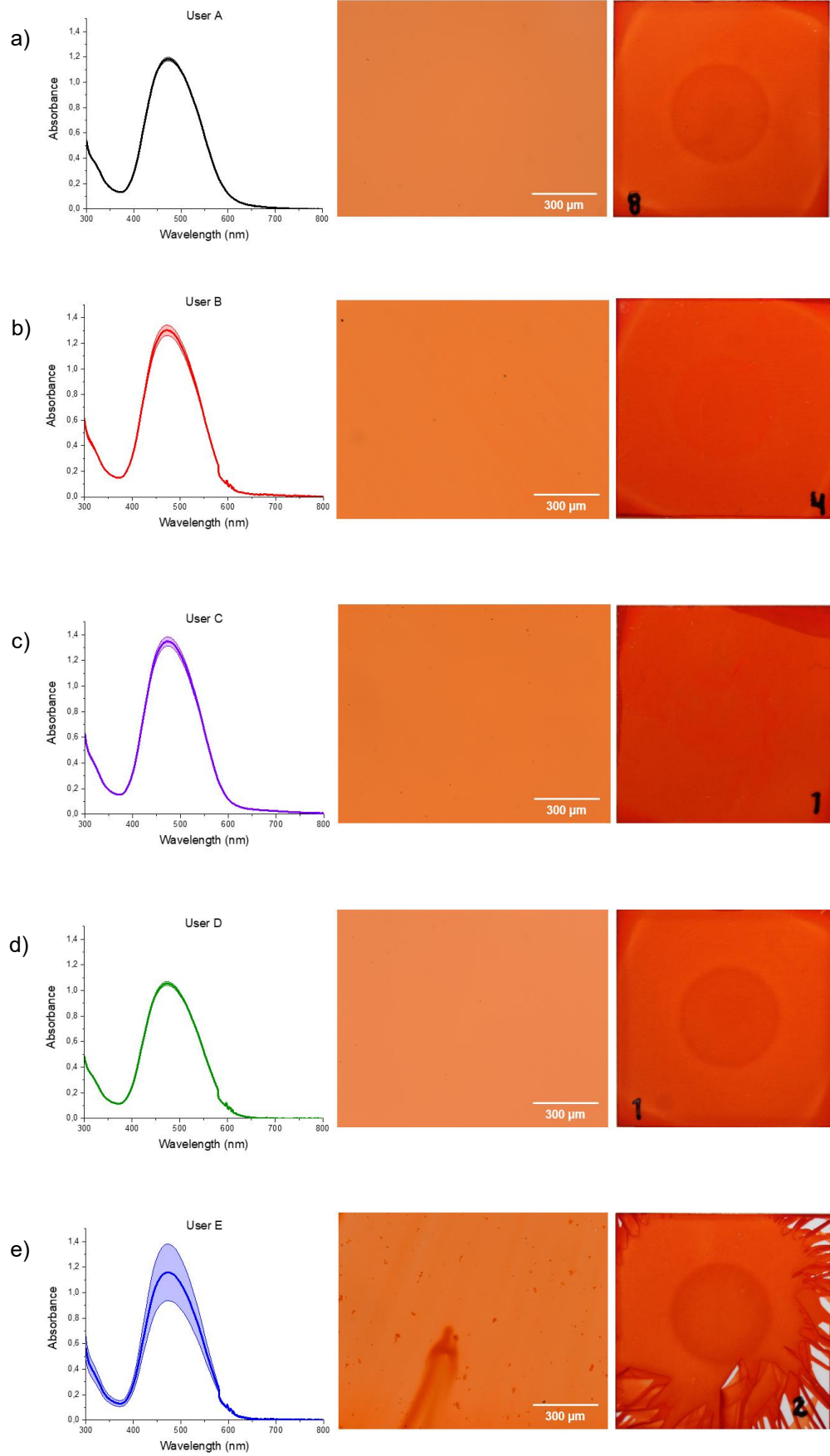**Figure 14.** *Samples made by different users with the new DR1-glass sample preparation protocol. The average absorption spectra, microscope images (scale bars: 300 µm) and single-lens camera images (sample size: 22×22 mm).* **a)** *Data of user A's samples.* **b)** *Data of user B's samples.* **c)** *Data of user C's samples.* **d)** *Data of user D's samples.* **e)** *Data of user E's samples.*

There are notable differences between the samples made by different people. Users A, B, C and D had previous experience of preparing samples by spin coating, meanwhile user E used a spin coater for the first time. The deviation in the absorption spectra of all the users with previous experience are moderately small, while the deviation of user E's samples is notable. User E's samples also contain swirls and splashes from dispensing the solution onto the substrate. This problem is typically eliminated when user becomes competent in spin coating. Thus, uniform, and reproducible sample preparation requires training and experience of the technique, while a person with plenty of experience of spin coating is able to produce moderately reproducible and uniform samples.

The maximum absorbance values of the users vary from one another, which can also be observed as differences in the sample colors. The differences are likely originating from sonication and filtration of DR1-glass solution. Users B and C reported that a lot of their solution was splattered to the walls and top of the vial while sonicating the solution. They also lost a part of the solution while filtering, and these two factors resulted in a prominent decrease in the volume of the solution. The aforementioned reasons along with evaporation of the solvent are likely to cause differences in the concentrations of the solutions. Each sample contained a darker circle in the middle, that was visible with a naked eye, but due to the camera settings, the circles are not visible in user B and C's samples which were darker than the rest.

Variation in the dispensing speed of the solution may be one of the factors causing differences between the samples made by different users – If the solution is added onto the rotating substrate more quickly, more of the solution is thrown from the substrate and the film ends up being thinner. Not only too fast or too slow, but also unsteady dispensing cause uneven areas in the spin coated film. Lastly, the distance of the pipette tip from the substate when dispensing affects the film quality. The best quality films are accomplished by dispensing the solution from about 1,5 cm distance of the substrate, yet the distance cannot be kept as a constant when spin coating by hand. Therefore, one way to improve both uniformity and reproducibility of the samples made by one or more users

is to use a pipette holder that keeps the distance between the pipette and the substate unchanged when preparing samples.

Since user dependency of the DR1-glass thin film preparation by spin coating is prominent, the only way to produce fully uniform and reproducible samples is by automatizing the preparation process. Addedly, as stated earlier in Section 2.3, the environmental factors also affect the quality of the film prepared by spin coating [9]. Therefore, fully uniform, reproducible samples are not achievable without control over the environmental factors, such as temperature and relative humidity of the laboratory premises where the samples are being prepared.

4.4.1 Scaling up the sample preparation process

Spin coating is an unsuitable option for sample preparation for large-scale manufacturing of samples due to user dependency but also relatively long preparation times and high levels of solution wastage. This limits the applications of spin coating to mainly research and development purposes. [17]

As stated in Section 2.2, slot-die coating is an easily scalable technique used for the preparation of highly uniform, thin films [17]. In slot-die coating, the solution is dispensed onto a substrate via a narrow slot close to the surface. The technique is used for preparing extremely uniform films with a thickness ranging from a few nanometers to several microns. [27] However, slot-die coating is a more complex technique compared to spin coating and the technique requires deep understanding and optimization of multiple parameters. This technique also requires more initial training and has very high initial setup cost compared to spin coating or other film preparation techniques. [17] All film preparation techniques have their advantages as well as disadvantages as well as requirements for the used material. Therefore, the technique for large-scale manufacturing of DR1-glass thin films need to be carefully considered before choosing a technique for prospective future scale-up and commercialization.

4.5 Cell culture

When manufacturing samples for cell culturing, there is always a concern whether the samples are cytotoxic or otherwise harmful to the cells. Thus, cytocompatibility of the samples were tested after the solvent was changed from chloroform to chloroform-1,2-dichloroethane blend, given that the hazard classifications of both chloroform and 1,2-dichloroethane are health hazard, irritant and toxic. Additionally, 1,2-dichloroethane is

classified to be carcinogenic, and chloroform has also been reported to be cytotoxic and cause carcinogenic effects in experimental animals. [28, 29].

Since both solvents are harmful to living organisms, it is inevitable to get rid of the solvents before using the samples in cell culture conditions. Thus, the samples were kept in a vacuum chamber at 65 °C for an hour after spin coating to ensure that the samples were dry, and the solvents had completely evaporated from the films.

Cytocompatibility of the samples was tested by culturing MDCK II cells on top of the DR1-glass films, and ultrasonicated coverslips were used as control samples. Before cell seeding, The DR1-glass samples and control glasses were coated with collagen I to enhance adhesion between cells and the material. The cells were cultured for 72 hours and were then fixed with PFA. After fixing, the cells were immunolabeled to study the cell morphology.

The morphology and junctions were studied based on biomarkers present in the cells. Herein, DAPI was used for staining the chromatin in cell nuclei for telling single cells apart. The cell-cell junctions were studied by detecting E-cadherin to see whether the cells form a tight and polarized epithelium. In addition, phalloidin was used for staining the actin fibers of the cells which are also involved in cell-cell junctions. Finally, phosphorylation of focal adhesion kinase indicates the formation of mature focal adhesions, and therefore phosphorylated FAK (pFAK) was used for studying the morphology of these adhesions within the cells. The immunolabeled cells were imaged with a confocal microscope and these images are presented in figure 15.
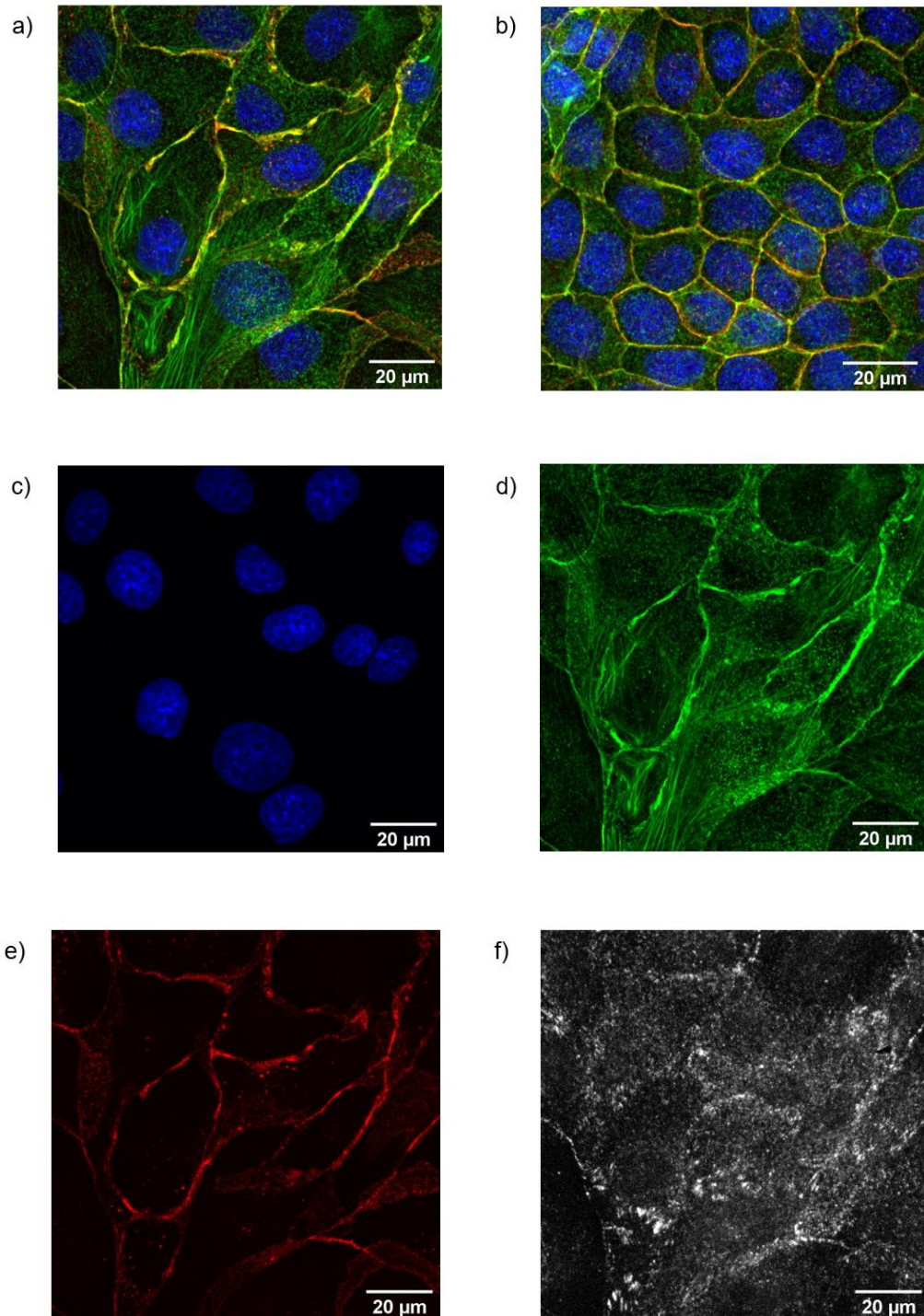
Figure 15. *Immunolabeled MDCK II cells on the samples after 72 h imaged with a confocal microscope. Scale bars: 20 µm.* **a)** *DR1-glass sample with DAPI, phalloidin and E-cadherin fluorescence channels.* **b)** *A control glass with DAPI, phalloidin and E-cadherin fluorescence channels.* **c)** *DR1-glass, cell nuclei stained with DAPI.* **d)** *DR1-glass, actin fibers stained with phalloidin.* **e)** *DR1-glass, cell-cell junction stained with E-cadherin.* **f)** *DR1-glass, focal adhesions stained with pFAK.*

Figure 15 shows that the cells growing on the DR1-glass look very different compared to the cells growing on the control glass. This difference in cell morphology originates from differences in the surface properties on the samples. Both topography and surface stiffness can affect the cell morphology and migration [30]. The cells on the control glass have already formed a tight, confluent monolayer typical for polarized epithelial cells. However, the cells layer on DR1-glass do not yet fill the whole sample surface. The cell morphology and visible actin fibers (green) reveal that these cells are still migrating on their growing platform.

E-cadherin strengthens the cell-cell junctions by linking to the actin cytoskeleton [31]. Accordingly, both actin fibers (green) and E-cadherin (red) at cell interface refer to strong cell-cell junctions on the DR1-glass. The morphology of the cells and a large amount of fluorescence from pFAK (grey) indicate that the cells are tightly adhered to the platform. The cell nuclei (blue) are spherical and intact, referring to good viability.

All in all, the morphology of the cells appears very promising. There are no visible signs of cytotoxicity even if the cell morphology differs from the control samples. Therefore, the cytocompatibility results indicate that usage of chloroform-1,2-dichloroethane blend in DR1-glass is not harmful for the cells, and there are no impediments for using the optimized solvent blend in light responsive cell culturing.

5. CONCLUSIONS AND FUTURE PROSPECTS

The aim of the thesis was to optimize DR1-glass thin films preparation protocol to produce high quality and reproducible samples for light-responsive cell culturing. The optimization included the solvent used for DR1-glass samples, preparation of the spin coating solution along with the parameters for the actual spin coating process.

The sample preparation protocol was modified by changing the solvent to chloroform-1,2-dichloroethane blend (80:20 % v/v) and the rotational speed of spin coating to 3000 rpm. The concentration of the DR1-glass solution was changed to 6 mg/µl. The glass substrates were washed by ultrasonication first in isopropanol and then in acetone. Further, sonication, filtration and heat treatment in a vacuum chamber were added to the preparation protocol.

The quality and appearance of the samples improved massively during optimization and variation between samples decreased considerably. The maximum standard error of the absorption spectra of the samples decreased by over 90 %. In addition, the visible swirls of material in the films were eliminated and the number of aggregates were decreased notably. Eventually, a person with plenty of experience of sample preparation by spin coating is able to produce reproducible and uniform samples by following the new, optimized DR1-glass thin films preparation protocol.

There are still a few sources of error in the DR1-glass thin films preparation protocol, which cause differences between the samples. The largest source of error is user-specific differences in sample preparation. In addition, the environmental factors and evaporation of the solvent cause minor variations in the samples prepared by spin coating. These error sources could be eliminated only by automizing the sample preparation process and controlling the environmental factors of the laboratory premises where samples are prepared.

The optimization results indicate that the DR1-glass samples are now uniform and reproducible enough for excluding sample dependences of cell behavior and detecting finer differences in cell-related parameters. Thus, these samples could be used in research of cell-material interactions along with cell behavior in dynamic environments.

The forthcoming step is to find a suitable protective layer material for the cell culture platform. The function of the layer is to prevent material dissolution in liquid environment and improve the cytocompatibility between the cells and the material. Here, DR1-glass itself is not considerably soluble or cytotoxic in cell culture environment, but the use of a

protective layer would allow the usage of other, more toxic or soluble, azo-materials in light-responsive cell culturing as well.

6. REFERENCES

[1]   Alberts, B. *et al.* (2018). *Essential Cell Biology*. 4th edition. New York, USA: Garland Publishing.

[2]   Yue B. (2014). 'Biology of the extracellular matrix: an overview'. *Journal of glaucoma*, 23(8 Suppl 1), pp. 20–23. Available at: https://doi.org/10.1097/IJG.0000000000000108 (Accessed: 28.11.2021)

[3]   Isomäki, M. *et al.* (2021). 'Light responsive bilayer cell culture platform for reversible cell guidance'. *Small Science*, online version before inclusion in an issue 2100099. Available at: http://doi.org/10.1002/smsc.202100099 (Accessed: 21.12.2021)

[4]   Mirbagheri, M. *et al.* (2019). 'Advanced cell culture platforms: a growing quest for emulating natural tissues'. *Materials Horizons,* 6(1), pp. 45-71. Available at: https://doi.org/10.1039/C8MH00803E (Accessed: 28.11.2021)

[5]   Municoy, S. *et al.* (2020). 'Stimuli-Responsive Materials for Tissue Engineering and Drug Delivery'. *International Journal of Molecular Sciences*, 21(13), pp. 4724. Available at: https://doi.org/10.3390/ijms21134724 (Accessed: 28.11.2021)

[6]   Fedele, C. *et al.* (2018). 'Azobenzene-baser polymers: emerging applications as cell culture platforms'. *Biomaterials Science,* 6(5), pp. 990-995. Available at: https://doi.org/10.1039/C8BM00019K (Accessed: 28.11.2021)

[7]   Kim, J., & Hayward, R. C. (2012). 'Mimicking dynamic *in vivo* environments with stimuli-responsive materials for cell culture'. *Trends in Biotechnology,* 30(8), pp. 426-439. Available at: https://doi.org/10.1016/j.tibtech.2012.04.003. (Accessed: 28.11.2021)

[8]   Priimägi, A., Shevchenko, A. (2014). 'Azopolymer-based micro- and nanopatterning for photonic applications'. *Journal of Polymer Science Part B: Polymer Physics*, *52*(3), pp. 163-182. Available at: https://doi.org/10.1002/polb.23390 (Accessed: 29.11.2021)

[9]   Griffin, J. *et al. Spin coating: Complete Guide to Theory and Techniques/Ossila* [Online]. Available at: https://www.ossila.com/pages/spin-coating (Accessed: 29.11.2021)

[10]   Priimägi, A. (2009). 'Polymer-azobenzene complexes: From supramolecular concepts to efficient photoresponsive polymers'. Doctoral dissertation. Helsinki University of Technology. Espoo, Finland.

[11]   Merino, E., Ribagorda, M. (2012). 'Control over molecular motion using the *cis-trans* photoisomerization of the azo group'. *Beilstein journal of organic chemistry*, 8, pp. 1071–1090. Available at: https://doi.org/10.3762/bjoc.8.119 (Accessed: 29.11.2021)

[12]   Ahmed, Z. *et al.* (2017). 'Controlling azobenzene photoswitching though combiner ortho-fluorination and -amination'. *Chemical Communications*, 53, pp.

12520-12523. Available at: https://doi.org/10.1039/C7CC07308A (Accessed: 29.11.2021)

[13]   *DR1-glass/Solaris Chem* [Online]. Available at: https://solarischem.com/prod-uct/dr1-glass-sol80485 (Accessed: 29.11.2021)

[14]   Kirby, R. *et al.* (2013). 'Disperse and disordered: a mexylaminotriazine-substi-tuted azobenzene derivative with superior glass and surface relief grating for-mation'. *Journal of Materials Chemistry C*, 2, pp. 841-847. Available at: https://doi.org/10.1039/C3TC32034K (Accessed: 29.11.2021)

[15]   Natasohn, A., Rochon, P. (2002). 'Photoinduced Motions in Azo-Containing Pol-ymers'. *Chemical Reviews,* 102(11), pp. 4139-4176. Available at: https://doi.org/10.1021/cr970155y (Accessed: 29.11.2021)

[16]   Rianna, C. *et al.* (2015). 'Reversible Holographic Patterns on Azopolymers for Guiding Cell Adhesion and Orientation'. *ACS Applied Materials & Interfaces*, 7(31), pp. 17984-16991. Available at: https://doi.org/10.1021/acsami.5b02080 (Accessed: 29.11.2021)

[17]   O'Kane, M. *Solution-Processing Techniques: A Comparison/Ossila* [Online]. Available at: https://www.ossila.com/pages/solution-processing-techniques-com-parison (Accessed: 29.11.2021)

[18]   Birnie, D. (2001). 'Rational solvent selection strategies to combat striation for-mation during spin coating of thin films'. *Journal of Materials Research*, 16(4), pp. 1145-1154. Available at: https://doi.org/10.1557/JMR.2001.0158 (Accessed: 21.12.2021)

[19]   Pollard, T. & Cooper, J. (2009). 'Actin, a central player in cell shape and move-ment'. *Science*, 326(5957), pp. 1208–1212. Available at: https://doi.org/10.1126/science.1175862 (Accessed 29.11.2021)

[20]   Gumbiner, B. (2005). 'Regulation of cadherin-mediated adhesion in morphogen-esis'. *Nature Reviews Molecular cell biology,* 6(8), pp. 622-634. Available at: https://doi.org/10.1038/nrm1699 (Accessed 29.11.2021)

[21]   Teixeira, A. *et al.* (2003). 'Epithelial contact guidance on well-defined micro- and nanostructured substrates'. *Journal of Cell Science*, 116(10), pp. 1881-1892. Available at: https://doi.org/10.1242/jcs.00383 (Accessed: 29.11.2021)

[22]   Hao Y. *et al.* (2017). 'Photo-responsive polymer materials for biological applica-tions'. *Chinese Chemical Letters*, 28(11), pp. 2085-2091. Available at: https://doi.org/10.1016/j.cclet.2017.10.019 (Accessed: 30.11.2021)

[23]   Homma, K. *et al.* (2021). 'Design of azobenzene-bearing hydrogel with pho-toswitchable mechanics driven by photo-induced phase transition for *in vitro* dis-ease modeling'. *Acta Biomaterialia*, 132, pp. 103-113. Available at: https://doi.org/10.1016/j.actbio.2021.03.028 (Accessed; 30.11.2021)

[24]   Fedele, C. *et al.* (2017). 'Azopolymer photopatterning for directional control of angiogenesis'. *Acta Biomaterialia,* 63, pp. 317-325. Available at: https://doi.org/10.1016/j.actbio.2017.09.022 (Accessed: 30.11.2021)

[25]   (2019). *How do I improve my spin coatings/Laurell Technologies Corporation* [Online]. Available at: http://www.spincoater.com/improve-my-spin-coating.php (Accessed: 29.11.2021)

[26]   Lim, Y. *et al.* (2021). 'A Field Guide to Azopolymeric Optical Fourier Surfaces and Augmented Reality'. *Advanced Functional Materials*, 31(39). Available at: https://doi.org/10.1002/adfm.202104105 (Accessed: 29.11.2021)

[27]   *Slot-die coating: Theory, Design & Applications/Ossila* [Online]. Available at: https://www.ossila.com/pages/slot-die-coating-theory (Accessed: 29.11.2021)

[28]   Foxall, K. (2007). *Chloroform Toxicological overview (1st version)/Health Protection Agency* [Online]. Available at: https://assets.publishing.service.gov.uk/government/uploads/system/uploads/attachment_data/file/338535/Chloroform_Toxicological_Overview.pdf (Accessed: 29.11.2021)

[29]   (2010). *Safety Data Sheet: 1,2-dichloroethane/Thermo Fisher Scientific* [Online]. Available at: https://www.fishersci.com/store/msds?partNumber=E175500&productDescription=1%2C2-DICHLOROETHAN+CR+ACS+500ML&vendorId=VN00033897&countryCode=US&language=en (Accessed 29.11.2021)

[30]   Monteiro, I. *et al.* (2018). 'Engineered systems to study the synergistic signaling between integrin-mediated mechanotransduction and growth factors (Review)'. *Biointerphases*, 13(6), 06D302. Available at: https://doi.org/10.1116/1.5045231 (Accessed: 30.11.2021)

[31]   Garcia, M. *et al.* (2018). 'Cell-Cell Junctions Organize Structural and Signaling Networks'. *Cold Spring Harbor perspectives in biology*, 10(4), a029181. Available at: https://doi.org/10.1101/cshperspect.a029181 (Accessed: 29.11.2021)

ATTACHMENT 1.

Optimized preparation protocol for thin DR1-glass films

Working stages

1. Clean a needed amount of 22×22 mm cover slips

    a. Ultrasonicate the coverslips in isopropanol for 10 min, temp --, freq 37.

    b. Ultrasonicate the coverslips in acetone for 10 min, temp --, freq 37.

    c. If needed, remove dust and other particles with compressed air.

    d. Make sure the cover slips are completely dry before spin coating.

2. Prepare 6 wt-% DR1-glass (SOL80485) solution in chloroform-1,2-dichloro-ethane (80:20 % v/v)

    a. Use compressed air for removing dust from two 4 ml glass vials with screw tops.

    b. Weight a needed amount of DR1-glass into one of the vials. Note: Do the solution for max. 10 samples at a time, since the evaporation of the solvents will cause variation in the concentration of the solution. Prepare solution enough for a few extra samples, since some of the solution might be lost during the preparation process.

    c. Calculate the needed amount of the solvents and pipette into the vial with DR1-glass. Mix gently with a rotational movement. Keep the vial open only when necessary to prevent the solvents from evaporating.

    d. Ultrasonicate the solution in a closed vial for 2 min, temp 45, freq 37. Let the solution to cool down to room temperature before opening the vial.

    e. Filter the solution with PTFE 0,2 µm (d=13mm) filter into the other vial (a 2 ml syringe and a needle are also needed).

    f. Ultrasonicate the solution in a closed vial for 2 min, temp 45, freq 37. Let the solution to cool down to room temperature before opening the vial.

3. Spin coating; 35 µl, rpm 3000, acel 1000, time 35 s, dynamic dispensing

   a. Use a 200 µl pipette with solvent safe pipette tips.

   b. Keep the vial open only when necessary to reduce evaporation.

   c. Make sure the cover slip is in the middle of the chuck adapter and vacuum is on, open the vial and keep the pipette tip in the solution for about 5 seconds (halogenated solvents swell up tips made of PP, which reduces the dripping of the solution when dispensing).

   d. Turn on the spinning and quickly but carefully dispense 35 µl of the solution onto the spinning cover slip.

      i. Use the index and middle fingers of your free hand to stabilize the pipette.

      ii. Keep the pipette in a vertical position.

      iii. Keep the pipette tip in about 1,5 cm distance from the center of the cover slip when dispensing.

      iv. Press the piston almost but now all the way to the end (air flow from the very end of dispensing will cause the film to be uneven from the center).

   e. Repeat until you have a needed number of samples.

4. Keep the samples in a vacuum chamber at 65 °C for 60 min to ensure that the solvents have completely evaporated.

5. Check the quality of your samples with a polarized light microscope and a UV-vis spectrophotometer.